Journal of Medicinal Chemistry

Article

pubs.acs.org/jmc

Synthesis and Biological Evaluation of 2-(Alkoxycarbonyl)-3-Anilinobenzo[*b*]thiophenes and Thieno[2,3-*b*]pyridines as New Potent Anticancer Agents

Romeo Romagnoli,*[,†] Pier Giovanni Baraldi,*[,†] Maria Kimatrai Salvador,[†] Delia Preti,[†] Mojgan Aghazadeh Tabrizi,[†] Marcella Bassetto,[†] Andrea Brancale,[†] Ernest Hamel,[§] Ignazio Castagliuolo,[∥] Roberta Bortolozzi,[⊥] Giuseppe Basso,[⊥] and Giampietro Viola*[,⊥]

[†]Dipartimento di Scienze Farmaceutiche, Università di Ferrara, 44121 Ferrara, Italy

[†]School of Pharmacy and Pharmaceutical Sciences, Cardiff University, King Edward VII Avenue, Cardiff CF10 3NB, United Kingdom

[§]Screening Technologies Branch, Developmental Therapeutics Program, Division of Cancer Treatment and Diagnosis, Frederick National Laboratory for Cancer Research, National Cancer Institute, National Institutes of Health, Frederick, Maryland 21702, United States

[∥]Dipartimento di Medicina Molecolare, Università di Padova, 35121 Padova, Italy

[⊥]Laboratorio di Oncoematologia, Dipartimento di Salute della Donna e del Bambino, Università di Padova, 35128 Padova, Italy

Supporting Information

ABSTRACT: Two new series of inhibitors of tubulin polymerization based on the 2-(alkoxycarbonyl)-3-(3′,4′,5′-trimethoxyanilino)benzo[*b*]thiophene and thieno[2,3-*b*]pyridine molecular skeletons were synthesized and evaluated for antiproliferative activity on a panel of cancer cell lines, inhibition of tubulin polymerization, cell cycle effects, and in vivo potency. Antiproliferative activity was strongly dependent on the position of the methyl group on the benzene portion of the benzo[*b*]thiophene nucleus, with the greatest activity observed when the methyl was located at the C-6 position. Also, in the smaller thieno[2,3-*b*]pyridine series, the introduction of the methyl group at the C-6 position resulted in improvement of antiproliferative activity to the nanomolar level. The most active compounds (**4i** and **4n**) did not induce cell death in normal human lymphocytes, suggesting that the compounds may be selective against cancer cells. Compound **4i** significantly inhibited in vivo the growth of a syngeneic hepatocellular carcinoma in Balb/c mice.

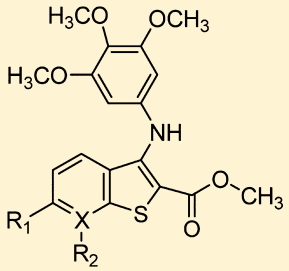

X=C or N
R_1=CH_3 or OCH_3
R_2=OCH_3 for X=C

INTRODUCTION

Microtubules are key components of the cytoskeleton of a eukaryotic cell and play an important role in a variety of essential cellular processes, such as mitotic spindle assembly during cell division, formation and maintenance of cell shape, regulation of motility, cell signaling, secretion, and intracellular transport.[1,2] Perhaps because of their significant role in cellular functions, microtubules are a proven molecular target for cancer chemotherapeutic agents.[3−5] Such compounds interfere with microtubule dynamics, which are particularly important during formation and functioning of the mitotic spindle required for proper chromosomal separation during cell division.[6] In the past few decades, a large number of small molecules displaying wide structural diversity and derived from natural sources or obtained by chemical synthesis have been identified and shown to interfere with the tubulin system.[7,8] Among the naturally occurring derivatives, combretastatin A-4 (CA-4, **1**; Chart 1), isolated from the bark of the South African tree *Combretum caffrum*, is one of the well-known tubulin-binding molecules affecting microtubule dynamics.[9] CA-4 strongly binds to the colchicine site of tubulin and prevents the polymerization of tubulin into microtubules.[10] CA-4 shows potent cytotoxicity against a wide variety of human cancer cells, including those that are multi-drug-resistant.[11] However, the low water solubility of **1** limited its efficacy in vivo, and a water-soluble disodium phosphate derivative of **1** (named combretastatin A-4 phosphate, CA-4P) has shown promising results in human cancer clinical trials.[12]

Anticancer therapy based on the discovery and development process of synthetic small molecules as inhibitors of tubulin assembly has interested us and many others in the past few years. In a recent study, we reported the synthesis and biological characterization of a class of molecules with general structure **2** that incorporated the structural motif of the 2-(3,4,5-trimethoxybenzoyl)-3-anilinobenzo[*b*]thiophene nucleus.[13] The most promising derivative in this collection (**2a**) was active at micromolar concentrations (IC_{50} =0.2−1.4 μM) as an antiproliferative agent in a panel of five cancer cell lines and weakly inhibited tubulin assembly, with activity 7-fold reduced relative to that of CA-4 (IC_{50} = 7.2 μM). Silvestri and co-workers reported a series of 2-(alkoxycarbonyl)-3-[(3,4,5-

Received: January 9, 2013
Published: February 28, 2013

   dx.doi.org/10.1021/jm400043d | *J. Med. Chem.* 2013, 56, 2606−2618

Chart 1. Chemical Structures of CA-4, 2-(Alkoxycarbonyl)-3-(arylthio)indoles 3, 2-Anilinobenzo[*b*]thiophenes 2a and 4a–k, and 2-Anilinothieno[2,3-*b*]pyridines 4l–n

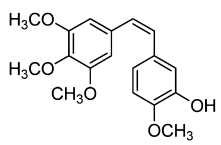

Combretastatin A-4 (CA-4), **1**

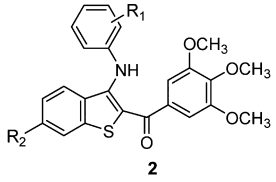

2

R_1=H, Cl, CH_3, OCH_3 or OC_2H_5
R_2=H or Me
2a, R_1=4-OEt, R_2=CH_3

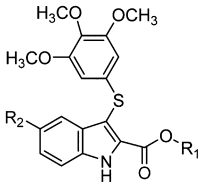

3

R_1=CH_3 or C_2H_5
R_2=H, Cl, Br or OCH_3

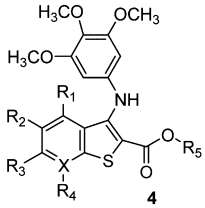

4

4a, X=C, $R_{1\text{-}4}$=H, R_5=CH_3
4b, X=C, $R_{1\text{-}4}$=H, R_5=C_2H_5
4c, X=C, $R_{1,5}$=CH_3, $R_{2\text{-}4}$=H
4d, X=C, R_1=CH_3, $R_{2\text{-}4}$=H, R_5=C_2H_5
4e, X=C, $R_{2,5}$=CH_3, $R_{1,3,4}$=H
4f, X=C, $R_{3,5}$=CH_3, $R_{1,2,4}$=H
4g, X=C, R_3=CH_3, $R_{1,2,4}$=H, R_5=C_2H_5
4h, X=C, $R_{4,5}$=CH_3, $R_{1\text{-}3}$=H
4i, X=C, R_3=OCH_3, $R_{1,2,4}$=H, R_5=CH_3
4j, X=C, R_3=OCH_3, $R_{1,2,4}$=H, R_5=C_2H_5
4k, X=C, R_4=OCH_3, $R_{1\text{-}3}$, R_5=CH_3
4l, X=N, $R_{1\text{-}3}$=H, R_4=nothing, R_5=CH_3
4m, X=N, $R_{1\text{-}3}$=H, R_4=nothing, R_5=C_2H_5
4n, X=N, $R_{3,5}$=CH_3, $R_{1,2}$=H, R_4=nothing

trimethoxyphenyl)thio]-5-substituted indoles with general structure **3**, with excellent activity as inhibitors both of tubulin polymerization and of the growth of MCF-7 human breast carcinoma cells.[14–16]

Since the 3,4,5-trimethoxyphenyl substituent was demonstrated to be the essential structural requirement for optimal biological activity in numerous tubulin inhibitors,[17,18] in an effort to further improve the activity of compound **2a**, we have explored the possibility of replacing the 3,4,5-trimethoxybenzoyl and substituted 4-ethoxyanilino moieties at the 2- and 3-positions of the benzo[*b*]thiophene nucleus of derivative **2a** with alkoxycarbonyl and 3,4,5-trimethoxyanilino functions, respectively, in an effort to enhance the activity of **2a** analogues. This provided a new series of 2-(methoxy/ethoxycarbonyl)-3-(3,4,5-trimethoxyanilino)benzo[*b*]thiophene derivatives (**4a–k**), modified with respect to position C-4 to C-7 with methyl or methoxy substitution, corresponding to compounds **4c–h** and **4i,k**, respectively. In addition, we explored the effect of bioisosteric replacement of the C-7 carbon of derivatives **4a**, **4b**, and **4f** with a basic nitrogen atom to furnish the 2-(alkoxycarbonyl)-3-(3,4,5-trimethoxyanilino)thieno[2,3-*b*]-pyridine derivatives **4l**, **4m**, and **4n**, respectively.

We examined the efficacy of the newly synthesized compounds with tubulin and on a panel of human cancer cell lines, including multi-drug-resistant lines overexpressing the 170 kDa P-glycoprotein drug efflux pump. To evaluate further the cytotoxicity of these compounds, we also determined their activity in normal human lymphocytes. Finally, with one of our most active compounds (**4i**) we obtained preliminary in vivo data with a syngeneic murine tumor model that indicated high activity in tumor growth suppression.

CHEMISTRY

The 2-(alkoxycarbonyl)-3-(3,4,5-trimethoxyanilino)benzo[*b*]-thiophenes **4a–k** and the corresponding thieno[2,3-*b*]pyridines **4l–n** were prepared through the three-step synthesis shown in Scheme 1. The condensation of 2-nitrobenzonitriles **5a–g** or 2-chloro-3-cyanopyridines **5h,i** with methyl/ethyl thioglycolate in DMF with aqueous KOH as the base furnished the 2-(methoxy/ethoxycarbonyl)-3-aminobenzo[*b*]thiophenes **6a–k** and the related thieno[2,3-*b*]pyridines **6l–n**, respectively, in good yields.[19] These latter compounds were transformed by substitutive deamination with *t*BuONO and $CuBr_2$ into the 3-bromobenzo[*b*]thiophenes **7a–k** and 3-bromothieno[2,3-*b*]-pyridines **7l–n**, respectively.[20]

The novel 2-(alkoxycarbonyl)-3-(3,4,5-trimethoxyanilino)-benzo[*b*]thiophenes **4a–k** and the corresponding thieno[2,3-*b*]pyridines **4l–n** were prepared by C–N palladium-catalyzed cross-coupling arylamination conditions of the appropriate 3-bromo derivatives **7a–n** with 3,4,5-trimethoxyaniline in the presence of $Pd(OAc)_2$, BINAP as the ligand, and $CsCO_3$ as the base in toluene.[21]

Scheme 1[a]

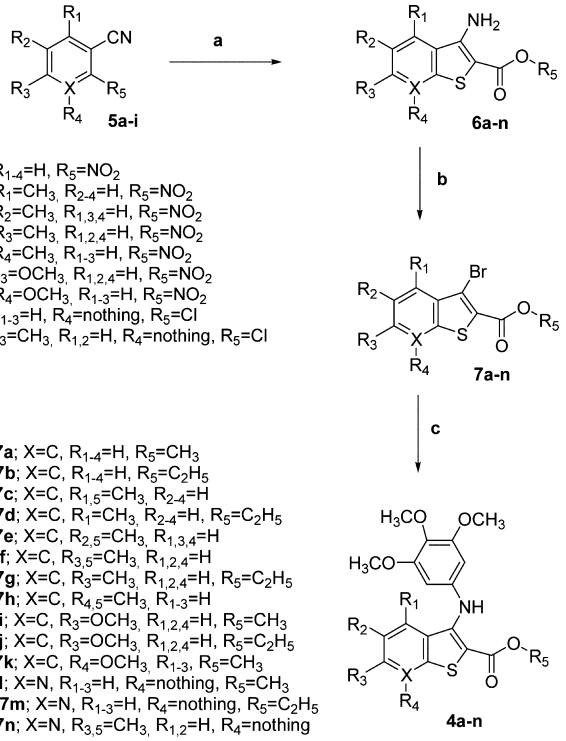

5a, X=C, $R_{1\text{-}4}$=H, R_5=NO_2
5b, X=C, R_1=CH_3, $R_{2\text{-}4}$=H, R_5=NO_2
5c, X=C, R_2=CH_3, $R_{1,3,4}$=H, R_5=NO_2
5d, X=C, R_3=CH_3, $R_{1,2,4}$=H, R_5=NO_2
5e, X=C, R_4=CH_3, $R_{1\text{-}3}$=H, R_5=NO_2
5f, X=C, R_3=OCH_3, $R_{1,2,4}$=H, R_5=NO_2
5g, X=C, R_4=OCH_3, $R_{1\text{-}3}$=H, R_5=NO_2
5h X=N, $R_{1\text{-}3}$=H, R_4=nothing, R_5=Cl
5i, X=N, R_3=CH_3, $R_{1,2}$=H, R_4=nothing, R_5=Cl

4a, 6-7a; X=C, $R_{1\text{-}4}$=H, R_5=CH_3
4b, 6-7b; X=C, $R_{1\text{-}4}$=H, R_5=C_2H_5
4c, 6-7c; X=C, $R_{1,5}$=CH_3, $R_{2\text{-}4}$=H
4d, 6-7d; X=C, R_1=CH_3, $R_{2\text{-}4}$=H, R_5=C_2H_5
4e, 6-7e; X=C, $R_{2,5}$=CH_3, $R_{1,3,4}$=H
4f, 6-7f; X=C, $R_{3,5}$=CH_3, $R_{1,2,4}$=H
4g, 6-7g; X=C, R_3=CH_3, $R_{1,2,4}$=H, R_5=C_2H_5
4h, 6-7h; X=C, $R_{4,5}$=CH_3, $R_{1\text{-}3}$=H
4i, 6-7i; X=C, R_3=OCH_3, $R_{1,2,4}$=H, R_5=CH_3
4j, 6-7j; X=C, R_3=OCH_3, $R_{1,2,4}$=H, R_5=C_2H_5
4k, 6-7k; X=C, R_4=OCH_3, $R_{1\text{-}3}$, R_5=CH_3
4l, 6-7l; X=N, $R_{1\text{-}3}$=H, R_4=nothing, R_5=CH_3
4m, 6-7m; X=N, $R_{1\text{-}3}$=H, R_4=nothing, R_5=C_2H_5
4n, 6-7n; X=N, $R_{3,5}$=CH_3, $R_{1,2}$=H, R_4=nothing

[a]Reagents and conditions: (a) $SHCH_2CO_2CH_3$ or $SHCH_2CO_2C_2H_5$, KOH, H_2O, DMF; (b) *t*BuONO, $CuBr_2$, CH_3CN, 65 °C; (c) 3,4,5-trimethoxyaniline, $Pd(OAc)_2$, BINAP, $CsCO_3$, PhMe, 120 °C, 16 h.

BIOLOGICAL RESULTS AND DISCUSSION

In Vitro Antiproliferative Activities. The 2-(methoxy/ethoxycarbonyl)-3-(3,4,5-trimethoxyanilino)benzo[*b*]-thiophenes **4a–k** and the related thieno[2,3-*b*]pyridines **4l–n** were evaluated for their antiproliferative activity against a panel of seven human cancer cell lines and compared with the reference compound **1** (Table 1).

Compounds with a methyl (**4f** and **4g**) or a methoxy (**4i** and **4j**) substituent at the C-6 position of the 2-(methoxy/

dx.doi.org/10.1021/jm400043d | *J. Med. Chem.* 2013, 56, 2606–2618

Table 1. In Vitro Cell Growth Inhibitory Effects of Compounds 4a−n and CA-4 (1)

	IC_{50}[a] (nM)						
compd	HeLa	A549	HL-60	Jurkat	SEM	MCF-7	HT-29
4a	427 ± 51	2850 ± 235	1536 ± 378	490 ± 53	179 ± 41	795 ± 42	299 ± 31
4b	3095 ± 200	8531 ± 2088	5491 ± 379	3023 ± 423	1901 ± 215	6391 ± 659	1610 ± 86
4c	1301 ± 248	4578 ± 588	3385 ± 342	6710 ± 1532	2505 ± 332	8192 ± 1135	1024 ± 197
4d	2520 ± 184	6252 ± 1555	7385 ± 1197	5666 ± 950	1933 ± 234	4153 ± 404	3614 ± 254
4e	398 ± 75	2806 ± 452	4717 ± 460	727 ± 151	185 ± 27	540 ± 86	299 ± 46
4f	0.31 ± 0.02	10.8 ± 4.5	20.5 ± 9.1	0.6 ± 0.1	0.7 ± 0.1	1.2 ± 0.9	1.9 ± 0.94
4g	0.38 ± 0.04	7.2 ± 3.1	3.9 ± 1.1	0.4 ± 0.2	1.5 ± 0.4	9.0 ± 4.3	6.0 ± 3.0
4h	1730 ± 143	3931 ± 401	4266 ± 369	1630 ± 704	1628 ± 157	4548 ± 371	552 ± 148
4i	0.28 ± 0.01	8.5 ± 1.9	0.4 ± 0.10	1.7 ± 0.8	10.3 ± 5.6	0.7 ± 0.08	0.9 ± 0.04
4j	0.56 ± 0.06	8.9 ± 2.8	31.6 ± 8.4	3.3 ± 1.3	10.2 ± 4.6	5.6 ± 1.5	10.2 ± 3.2
4k	3.5 ± 1.1	33.0 ± 10.1	25.6 ± 8.0	56.5 ± 15.2	2.3 ± 0.6	95 ± 33.2	14.9 ± 3.9
4l	342 ± 42.2	3850 ± 316	2915 ± 882	1113 ± 176	348 ± 63	2644 ± 423	542 ± 130
4m	2102 ± 737	7157 ± 969	6097 ± 823	8450 ± 1520	1850 ± 248	5275 ± 736	2259 ± 475
4n	0.18 ± 0.05	16.2 ± 4.4	0.4 ± 0.08	0.6 ± 0.02	0.5 ± 0.01	0.53 ± 0.09	0.35 ± 0.15
CA-4	4 ± 1	180 ± 50	1 ± 0.2	5 ± 0.6	5 ± 0.1	370 ± 100	3100 ± 100

[a] IC_{50} = compound concentration required to inhibit tumor cell proliferation by 50%. Data are presented as the mean ± SE from the dose−response curves of at least three independent experiments.

ethoxycarbonyl)-3-(3,4,5-trimethoxyanilino)benzo[*b*]thiophene system, along with the 2-(methoxycarbonyl)-3-(3,4,5-trimethoxyanilino)-6-methylthieno[2,3-*b*]pyridine (**4n**), exhibited the greatest antiproliferative activity among the tested compounds, with IC_{50} values of 0.31−20, 0.38−9.0, 0.28−10, 0.56−32, and 0.18−16 nM, respectively, showing more activity against HeLa cells as compared with the other cell lines. Derivative **4n** was the only compound more potent than the reference compound **1** (from 1 to 3 orders of magnitude) against all cancer cell lines.

The two C-4/C-7-unsubstituted benzo[*b*]thiophene derivatives **4a** and **4b** proved moderately active, with **4a** being about 3−10-fold more active than **4b** (IC_{50} = 0.18−2.8 and 1.9−8.5 μM, respectively). The results presented in Table 1 show that the location of the methyl group on the benzene portion of the benzo[*b*]thiophene nucleus plays a critical role in inhibition of cell growth, with the greatest activity observed when the methyl is at the C-6 position of the benzo[*b*]thiophene nucleus (compounds **4f** and **4g**) (IC_{50} = 0.31−11 nM). Shifting the methyl group to the C-5 position (**4e**) resulted in only modest activity (IC_{50} = 0.18−2.8 μM), while moving it to either the C-4 or C-7 position further decreased activity (derivatives **4c**, **4d**, and **4h**, IC_{50} as high as 8.2 μM).

Comparing the two C-6 methyl analogues **4f** and **4g**, the activity of methoxycarbonyl compound **4f** was quite similar to that of the ethoxycarbonyl homologue **4g** against HeLa, A549, and Jurkat cells, while there were greater differences from the other cell lines. **4f** was 2−7-fold more active than **4g** against SEM, HT-29, and MCF-7 cells, while **4g** was 5-fold more potent than **4f** against HL-60 cells. With the exception of HL-60 cells, both these molecules were more potent than the positive control **1**.

As compounds **4i** and **4j** demonstrate, the C-6 methyl group can be replaced with a methoxy group without substantial loss of activity against HeLa, A549, MCF-7, and HT-29 cells. As growth inhibitors, **4i** and **4j** were equipotent against A549 and SEM cells, while the methoxycarbonyl derivative **4i** was from 2- to 10-fold more potent than its ethoxycarbonyl counterpart **4j** against the other five cancer cell lines. Although compound **4i** was 2-fold less potent than **1** against the SEM cells, it was 2−3000-fold more active than **1** against the other six cell lines.

Replacing the C-7 methyl group of compound **4h** with a methoxy moiety (**4k**) increased antiproliferative activity from 1 to 3 orders of magnitude (IC_{50} = 552−4548 and 2.3−95 nM for **4h** and **4k**, respectively), indicating that methyl and methoxy groups are not bioequivalent at the C-7 position of the benzo[*b*]thiophene nucleus.

A comparison between the methoxycarbonyl derivatives **4i** and **4k** demonstrated that the C-6 methoxy derivative **4i** was generally 1−2 orders of magnitude superior as an inhibitor of cancer cell growth relative to the C-7 methoxy analogue **4k**. The only exception was the SEM cells, which were somewhat more sensitive to **4k**.

Comparing the two unsubstituted 2-(alkoxycarbonyl)-3-(3,4,5-trimethoxyanilino)thieno[2,3-*b*]pyridine derivatives **4l** and **4m**, the methoxycarbonyl group on the C-2 position of thieno[2,3-*b*]pyridine analogue **4l** resulted in better inhibitory activity than the ethoxycarbonyl moiety of **4m**. As previously observed for the benzo[*b*]thiophene series, for the thieno[2,3-*b*]pyridine derivatives, the introduction of a methyl group at the C-6 position (compound **4n**) resulted in a dramatic reduction in IC_{50} values to nanomolar and subnanomolar levels. Comparing **4n** with the benzo[*b*]thiophene analogue **4f**, replacement of the benzene with the bioisosteric pyridine ring produced a 2−50-fold increase in activity against HeLa, HL-60, MCF-7, and HT-29 cells, while **4f** and **4n** were equipotent against Jurkat and SEM cells. Reduction in potency was observed only against A549 cells.

Evaluation of Cytotoxicity in Human Peripheral Blood Lymphocytes. To obtain more insight into the cytotoxic potential of these new compounds for normal human cells, two of the most active compounds (**4i** and **4n**) were assayed in vitro against peripheral blood lymphocytes (PBLs) from healthy donors (Table 2). Compounds **4i** and **4n** were ineffective in resting lymphocytes having an IC_{50} > 10 μM and proved cytotoxic only for PHA-stimulated PBLs, but at higher concentrations (2000−3000-fold) than those active against the lymphoblastic cell lines Jurkat and CEM. These data thus suggest that these compounds may have cancer cell selective killing properties.

Effect of Compounds 4i and 4n on Multi-Drug-Resistant Cells. Drug resistance is an important therapeutic

dx.doi.org/10.1021/jm400043d | J. Med. Chem. 2013, 56, 2606−2618

Table 2. Cytotoxicity of 4i and 4n for Human PBLs

	IC_{50}[a] (μM)	
cell line	**4i**	**4n**
$PBLs_{resting}$[b]	>10	>10
$PBLs_{PHA}$[c]	2.8 ± 1.2	3.4 ± 1.3

[a]IC_{50} = compound concentration required to reduce cell growth inhibition by 50%. Values are the mean ± SEM for three separate experiments. [b]PBLs not stimulated with PHA. [c]PBLs stimulated with PHA.

problem caused by the emergence of tumor cells possessing different mechanisms that confer resistance against a variety of anticancer drugs.[22,23] The more common mechanisms are those related to the overexpression of a cellular membrane protein called P-glycoprotein (P-gp) that mediates the efflux of various structurally unrelated drugs.[22,23] In this context, we evaluated the sensitivity of **4i** and **4n** on two multi-drug-resistant cell lines, one derived from lymphoblastic leukemia ($CEM^{Vbl-100}$), the other derived from colon carcinoma ($Lovo^{Doxo}$). Both these lines express high levels of P-gp.[24,25] As shown in Table 3, the

Table 3. In Vitro Cell Growth Inhibitory Effects of Compounds 4i and 4n on Drug-Resistant Cell Lines

	IC_{50}[a] (nM)		
compd	LoVo	$LoVo^{Doxo}$	resistance ratio[b]
4i	0.3 ± 0.1	0.4 ± 0.2	1.3
4n	1.9 ± 0.8	0.5 ± 0.2	0.3
doxorubicin	95.6 ± 43.2	11296 ± 356	118
	CEM	CEM^{Vbl100}	resistance ratio[b]
4i	3.2 ± 0.4	1.3 ± 0.1	0.4
4n	2.8 ± 0.2	4.2 ± 0.1	1.5
vinblastine	2.0 ± 0.5	211 ± 82	105
	A549	A549-T12	resistance ratio[b]
4l	8.5 ± 1.9	12.6 ± 2.9	1.5
4m	16.2 ± 4.4	19.5 ± 2.3	1.2
paclitaxel	3.5 ± 0.9	92.3 ± 26.8	26

[a]IC_{50} = compound concentration required to inhibit tumor cell proliferation by 50%. Data are presented as the mean ± SE from the dose–response curves of at least three independent experiments. [b]The values express the ratio between IC_{50} determined in resistant and nonresistant cell lines.

two compounds were equally potent toward parental cells and cells resistant to vinblastine or doxorubicin, showing a resistance index (RI, the ratio between IC_{50} values of resistant cells and sensitive cells) of about 1.

Resistance to microtubule inhibitors may also be mediated by changes in the levels of expression of different β-tubulin isotypes and by tubulin gene mutations.[26−28] Although a high rate of tubulin mutations have not been found in patients with different forms of tumors, this kind of mutation, when present, can result in modified tubulin with impaired polymerization properties and dynamics that probably lead to alterations in drug efficacy.

A-549-T12 is a cell line with an α-tubulin mutation with increased resistance to paclitaxel.[29] Compounds **4i** and **4n** had greater relative activity than paclitaxel in this cell line (Table 3), having an RI similar to that found in wild-type cells, suggesting that, in addition to classical resistance mediated by P-gp, these compounds might be useful in the treatment of tumors in which drug resistance involves tubulin mutations.

Inhibition of Tubulin Polymerization and Colchicine Binding. To investigate whether the antiproliferative activities of compounds **4f,g**, **4i−k**, and **4n** derived from an interaction with tubulin, these agents were evaluated for their inhibition of tubulin polymerization and for effects on the binding of [^{3}H]colchicine to tubulin (Table 4).[30−32] For comparison, CA-4 was examined in contemporaneous experiments. All tested compounds strongly inhibited tubulin assembly, and derivatives **4i**, **4j**, **4k**, and **4n**, with IC_{50} values of 0.88, 0.81, 0.76, and 0.70 μM, respectively, exhibited antitubulin activity greater than that of CA-4 (IC_{50} = 1.1 μM), while **4f** and **4g** had IC_{50} values of 1.2 and 1.1 μM, respectively, essentially equivalent to that of CA-4. Thus, the order of inhibitory effects on tubulin polymerization was **4n** > **4k** > **4j** > **4i** > CA-4 = **4g** > **4f**. With the exception of **4k**, there was an excellent correlation between inhibition of tubulin polymerization and antiproliferative activity.

Table 4. Inhibition of Tubulin Polymerization and Colchicine Binding by Compounds 4f,g, 4i−k, and 4n and CA-4

		colchicine binding[b] (%) ± SD	
compd	tubulin assembly[a] IC_{50} (μM) ± SD	5 μM drug	1 μM drug
4f	1.2 ± 0.05	95 ± 0.6	71 ± 2
4g	1.1 ± 0.09	89 ± 0.2	58 ± 0.5
4i	0.88 ± 0.1	98 ± 1	85 ± 2
4j	0.81 ± 0.06	94 ± 1	77 ± 0.6
4k	0.76 ± 0.02	76 ± 2	54 ± 1
4n	0.70 ± 0.01	95 ± 0.9	78 ± 2
CA-4 (**1**)	1.1 ± 0.1	99 ± 0.1	90 ± 1

[a]Inhibition of tubulin polymerization. Tubulin was at 10 μM. [b]Inhibition of [^{3}H]colchicine binding. Tubulin and colchicine were at 1 and 5 μM, respectively, and the tested compound was at the indicated concentration.

In the colchicine studies, compounds **4f,g**, **4i−k**, and **4n** potently inhibited the binding of [^{3}H]colchicine to tubulin, since 76−98% inhibition occurred with these agents and colchicine both at 5 μM. Compound **4i** was the most active inhibitor of the binding reaction, since 85% and 98% inhibition occurred with this agent at 1 and 5 μM, respectively. Compound **4i** was as active as CA-4 when both compounds were tested at 5 μM, while at 1 μM **4i** was slightly less potent than CA-4, which in these experiments inhibited colchicine binding by 99% and 90% at 5 and 1 μM, respectively.

While this group of compounds were all highly potent in the biological assays (inhibition of cell growth, tubulin assembly, and colchicine binding), correlation between the last two assay types was imperfect. Thus, while compound **4n** was the best inhibitor of tubulin assembly, its effect on colchicine binding was matched by that of derivative **4f**, which was 1.5-fold less active as an assembly inhibitor. In general, in these experiments inhibition of tubulin assembly correlated more closely with antiproliferative activity than did inhibition of [^{3}H]colchicine binding.

The results are consistent with the conclusion that the antiproliferative activity of these compounds derives from an interaction with the colchicine site of tubulin and interference with microtubule assembly.

Molecular Modeling. To investigate the possible binding mode for this series of compounds, we performed a series of molecular docking simulations on the colchicine site of

dx.doi.org/10.1021/jm400043d | J. Med. Chem. 2013, 56, 2606−2618

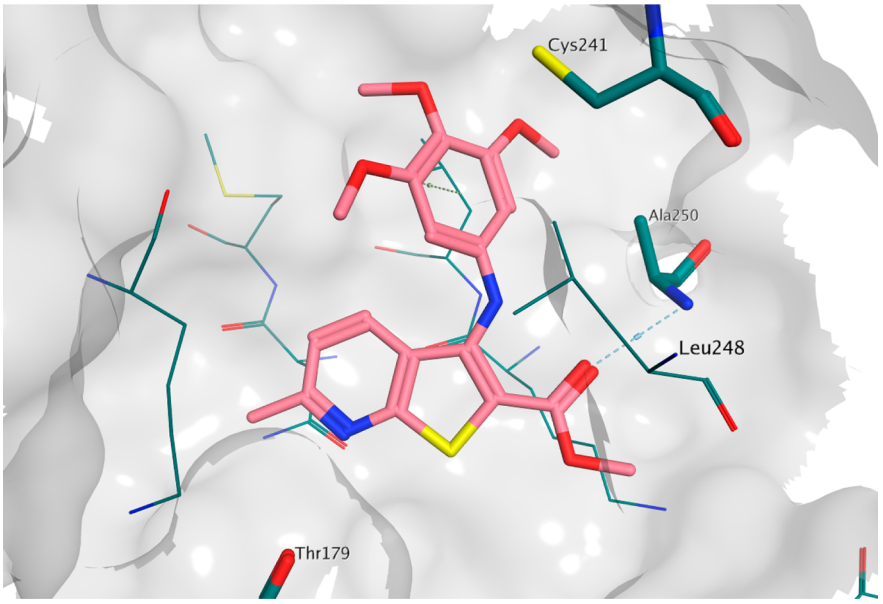

Figure 1. Binding model of **4n** in the colchicine site of tubulin. The hydrogen bond with βAla250 is indicated by a dashed line.

tubulin.[33] The results obtained are similar to those reported for the (arylthio)indole family (**3**),[34] with the trimethoxyphenyl ring in proximity of βCys241 and the heterocycle sitting deep in the hydrophobic pocket (Figure 1). However, the formation of an intramolecular hydrogen bond between the amino group and the carbonyl group in this series of compounds forces the ester moiety into a different orientation compared with that of **3**, and this allows the formation of a hydrogen bond between the ester itself and βAla250. Interestingly, this binding pose was observed for all the compounds in the reported series (see the Supporting Information, Figure 1s), although, in the case of **4h**, the methyl substituent induced a slight, yet significant, change in the pose orientation that caused the loss of the hydrogen bond described above (Figure 2). It should be noted that the

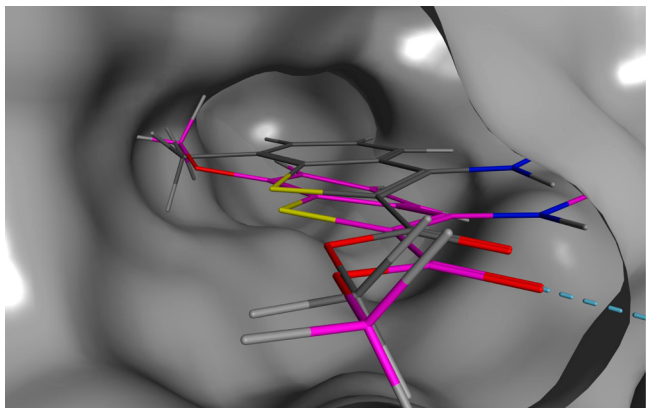

Figure 2. Binding poses of **4h** (in gray) and **4k** (in magenta) in the colchicine site of tubulin. The hydrogen bond between **4k** and βAla250 is indicated by a dashed line.

methoxy-substituted analogue **4k** was able to maintain the hydrogen bond between βAla250 and the ester group, suggesting that the binding pocket has very specific steric properties in this region, and this in turn suggests a structural justification for the loss of activity observed for **4h**.

Analysis of Cell Cycle Effects. The effects of 24 h treatment with different concentrations of **4i** and **4n** on cell cycle progression in Jurkat, HT-29, and HeLa cells were determined by flow cytometry (Figure 3). The two compounds caused a significant G2/M arrest in a concentration-dependent manner in the cell lines tested, with a rise in G2/M cells occurring at a concentration as low as 20 nM, while at higher concentrations more than 80% of the cells were arrested in G2/M. The cell cycle arrest in the G2/M phase was accompanied by a commensurate reduction in cells in the other phases of the cell cycle.

We next studied the association between **4i**-induced G2/M arrest and alterations in expression of proteins that regulate cell division. The cdc2/cyclin B complex controls both entry into and exit from mitosis. Phosphorylation of cdc2 on Tyr15 and phosphorylation of cdc25c phosphatase on Ser216 negatively regulate the activation of the cdc2/cyclin B complex.

Thus, dephosphorylation of these proteins is needed to activate the cdc2/cyclin B complex. Cdc25c is a major phosphatase that dephosphorylates the site on cdc2 and autodephosphorylates itself. Phosphorylation of cdc25C directly stimulates both its phosphatase and its autophosphatase activities, a condition necessary to activate cdc2/cyclin B on entry of cells into mitosis.[35−37] As shown in Figure 4 in HeLa cells, treatment with **4i** at either 10 or 100 nM caused no significant variations in cyclin B expression after either a 24 or 48 h treatment. In contrast, slower migrating forms of phosphatase cdc25c appeared at 24 and 48 h, indicating changes in the phosphorylation state of this protein. We also observed a dramatic decrease in the expression of the phosphorylated form of cdc2 (Tyr15). These data, along with the fact that over 80% of the cells accumulated in the G2/M phase, suggest that **4i**-induced G2/M arrest is not due to defects in G2/M regulatory proteins but, rather, is closely linked with acceleration of entry into mitosis.

Compounds 4i and 4n Induce Apoptosis. To characterize the mode of cell death induced by **4i** and **4n**, a biparametric cytofluorimetric analysis was performed using PI, which stains DNA and enters only dead cells, and fluorescent immunolabeling of the protein annexin-V, which binds to PS in a highly

dx.doi.org/10.1021/jm400043d | J. Med. Chem. 2013, 56, 2606−2618

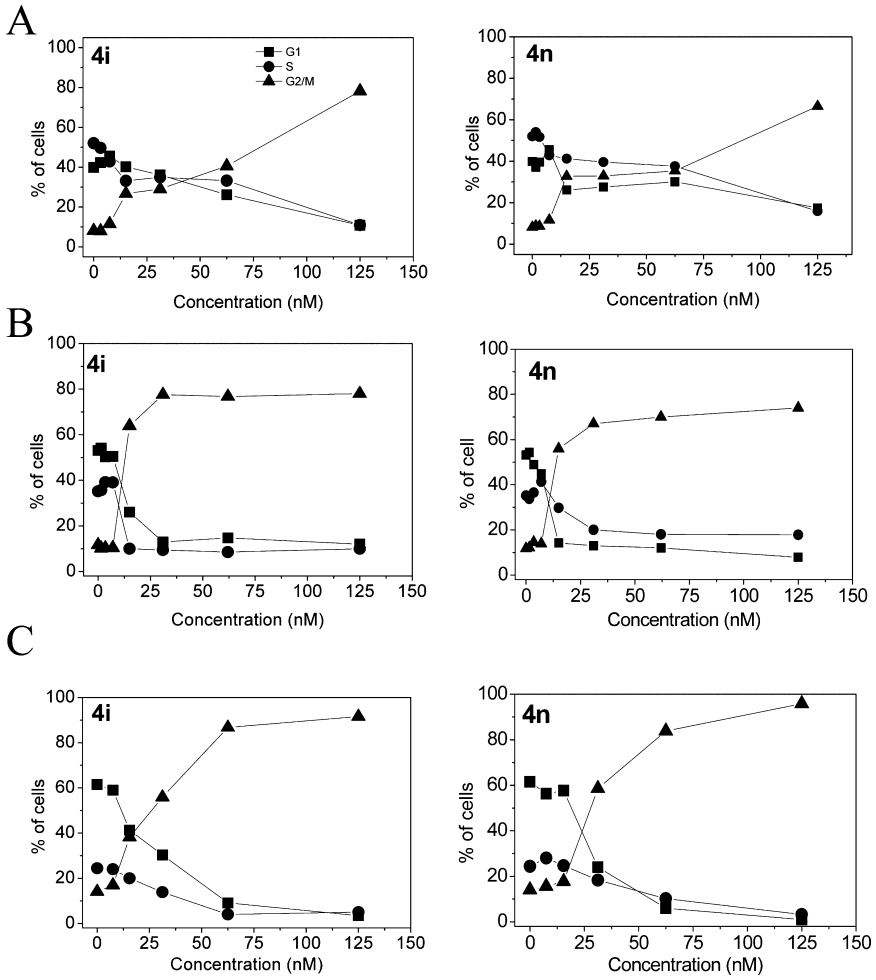

Figure 3. Percentage of cells in each phase of the cell cycle in Jurkat (A), HT29 (B), and HeLa (C) cells treated with the indicated compounds at the indicated concentrations for 24 h. Cells were fixed and labeled with PI and analyzed by flow cytometry as described in the Experimental Section.

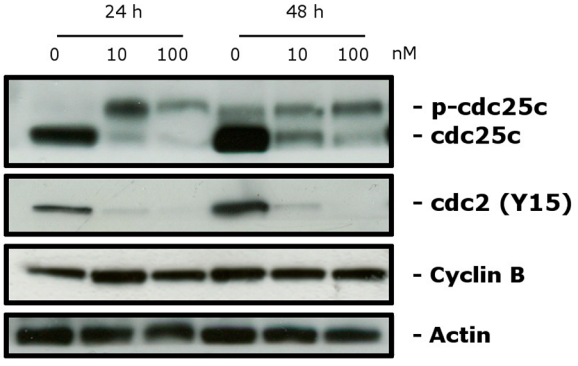

Figure 4. Effect of **4i** on G2/M regulatory proteins. HeLa cells were treated for 24 or 48 h with the indicated concentration of **4i**. The cells were harvested and lysed for the detection of cyclin B, p-cdc2^{Y15}, and cdc25C expression by Western blot analysis. To confirm equal protein loading, each membrane was stripped and reprobed with anti-β-actin antibody.

selective manner.[38] Dual staining for annexin-V and with PI permits discrimination among live cells (annexin-V$^-$/PI$^-$), early apoptotic cells (annexin-V$^+$/PI$^-$), late apoptotic cells (annexin-V$^+$/PI$^+$), and necrotic cells (annexin-V$^-$/PI$^+$). As depicted in Figure 5, HeLa cells treated with **4i** or **4n** showed an accumulation of annexin-V-positive cells in comparison with the control, in a concentration- and time-dependent manner.

Compounds 4i and 4n Induce Mitochondrial Dysfunction. Mitochondria play an essential role in the propagation of apoptosis.[39] It is well established that, at an early stage, apoptotic stimuli alter the mitochondrial transmembrane potential ($\Delta\psi_{mt}$). $\Delta\psi_{mt}$ was monitored by the fluorescence of the dye 5,5′,6,6′-tetrachloro-1,1′,3,3′-tetraethylbenzimidazolcarbocyanine (JC-1). As shown in Figure 6, both **4i** and **4n** induced a time- and concentration-dependent increase in the proportion of cells with depolarized mitochondria.

Mitochondrial membrane depolarization is associated with mitochondrial production of ROS.[40] Therefore, we investigated whether ROS production increased after treatment with **4i** or **4n**. We analyzed the production of ROS by flow cytometry utilizing two fluorescence indicators: hydroxyethydine (HE) or 2,7-dichlorodihydrofluorescein diacetate (H_2-DCFDA).[41]

The results presented in Figure 7 show that both **4i** and **4n** induced the production of significant amounts of ROS in comparison with control cells, which agrees with the previously described dissipation of $\Delta\psi_{mt}$. Altogether, these results indicate that these compounds induced apoptosis through the mitochondrial pathway. In this context, it is interesting to note that many other antimitotic compounds induce apoptosis through the mitochondrial pathway.[13,42]

Compound 4i Induces Caspase Activation. The activation of caspases plays a central role in the process of

dx.doi.org/10.1021/jm400043d | J. Med. Chem. 2013, 56, 2606−2618

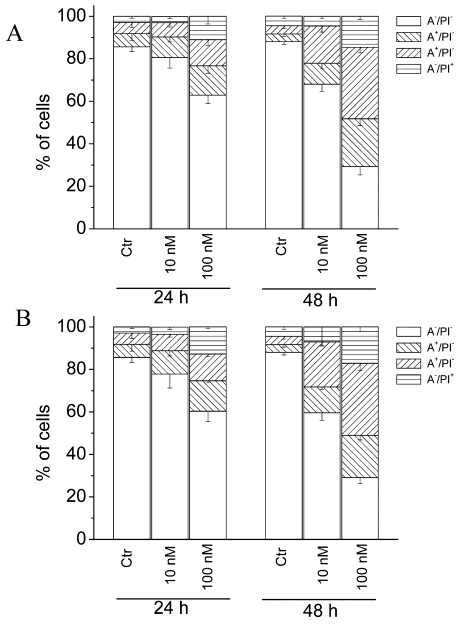

Figure 5. Flow cytometric analysis of apoptotic cells after treatment of HeLa cells with **4i** (A) or **4n** (B) at the indicated concentrations after incubation for 24 or 48 h. The cells were harvested and labeled with annexin-V−FITC and PI and analyzed by flow cytometry. Data are represented as the mean ± SEM of three independent experiments.

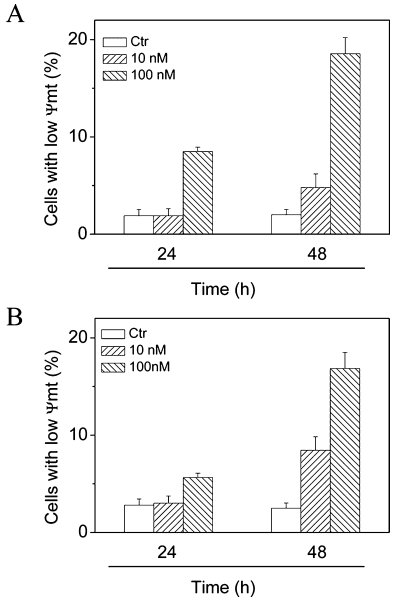

Figure 6. Assessment of mitochondrial membrane potential ($\Delta\psi_{mt}$) after treatment of HeLa cells with compound **4i** (A) or **4n** (B). Cells were treated with the indicated concentration of compound for 24 or 48 h and then stained with the fluorescent probe JC-1. Data are presented as the mean ± SEM for three independent experiments.

apoptotic cell death.[43] Synthesized as proenzymes, caspases are themselves activated by specific proteolytic cleavage reactions. Caspases-2, -8, -9, and -10 are termed initiator caspases and are usually the first to be activated in the apoptotic process. Following their activation, they in turn activate effector caspases, in particular caspase-3.[44] As shown in Figure 8A, compound **4i** induced proteolytic cleavage of caspase-9 and caspase-3, in good agreement with the mitochondrial depolarization described above. The DNA repair enzyme poly(ADP-ribose) polymerase (PARP) is cleaved by caspase-3 from its full-length 116 kDa form to an inactive 85 kDa form. We also observed that PARP cleavage was detectable at 24 h and at a low concentration (10 nM) of **4i**. Altogether, these results showed that **4i**-induced apoptosis is caspase-dependent, in addition to utilizing the intrinsic (mitochondrial) pathway.

Effect of 4i on Proapoptotic Proteins and IAP Expression. There is increasing evidence that regulation of the Bcl-2 family of proteins shares the signaling pathways induced by antimicrotubule compounds.[45] Several proapoptotic family proteins (e.g., Bax, Bid, Bim, and Bak) promote the release of cytochrome *c*, whereas antiapoptotic members (Bcl-2, Bcl-XL, Mcl-1) are capable of antagonizing the proapoptotic proteins and preventing the loss of mitochondrial membrane potential. Antimitotic drugs can induce the phosphorylation of Bcl-2 and Bcl-XL.[46] In agreement with these observations, we found that Bcl-XL was phosphorylated after treatment with **4i**, as demonstrated by a band shift (Figure 8B), and these results are in agreement with previous studies.[46] Mcl-1 is an antiapoptotic member of the Bcl-2 family, and recently it has been reported that sensitivity to antimitotic drugs is regulated by Mcl-1 levels.[47] As shown in Figure 8B, as with Bcl-XL, a slower migrating form of the Mcl-1 band appeared, indicative of Mcl-1 phosphorylation. This change was observed after 24 h treatments at both 10 and 100 nM **4i**, while the unmodified protein disappeared. In addition, a substantial reduction in the phosphorylated form occurred by 48 h with 10 nM **4i**. With 100 nM **4i**, there was much less phosphorylated Mcl-1 at 24 h than with 10 nM **4i**, suggesting that peak formation of phosphorylated Mcl-1 occurred even earlier. These results are in agreement with recent studies that underlined the importance of Mcl-1 phosphorylation and its subsequent degradation in response to antimitotic agents and that this event potentiates cell death.[48,49]

Xiap and survivin are members of the IAP family (inhibitors of apoptosis protein). In general, the IAPs function through direct interactions to inhibit the activity of several caspases, including caspase-3, caspase-7, and caspase-9, and they thereby inhibit the processing and activation of these enzymes.[50] Our results (Figure 8B) showed that expression of Xiap was almost eliminated after a 24 h treatment with **4i**, even at a concentration of 10 nM.

Of note, survivin was phosphorylated on Thr32 upon treatment with **4i** at both 24 and 48 h. This effect is consistent with cell cycle arrest in mitosis and is shared by various antimitotic drugs.[51,52]

In Vivo Antitumor Activity of Compound 4i. To evaluate the in vivo antitumor activity of **4i**, a syngeneic hepatocellular carcinoma model in mice was used.[53] It was established by subcutaneous injection of BNL 1ME A.7R.1 cells into the backs of Balb/c mice. In preliminary experiments in vitro, we determined that compound **4i** showed remarkable cytotoxic activity (IC_{50} = 2.1 nM) against BNL 1ME A.7R.1 cells. Once the BNL 1ME A.7R.1 allografts reached a size of ~100 mm^3, fifteen mice were randomly assigned to one of the three groups. In two of the groups, compound **4i** and the reference compound CA-4P, both dissolved in a 0.9% NaCl solution containing 5% polyethylene glycol 400 and 0.5% Tween 80, were injected intraperitoneally at a dose of 5 mg/kg, while the third group was used as a control. Both drugs, as well as the vehicle control, were administered daily for seven days. As shown in Figure 9A, compound **4i** immediately caused a significant reduction in tumor growth, and this reached a 68.5%

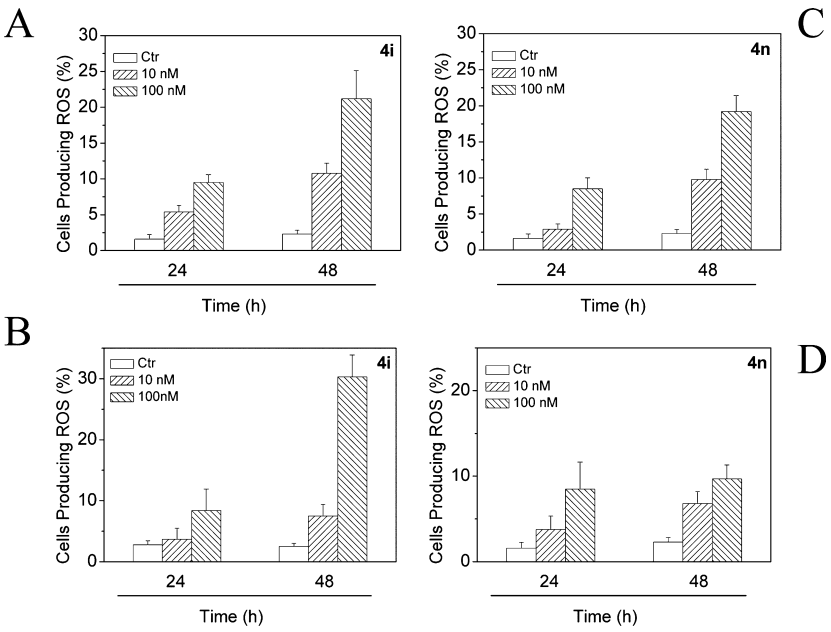

Figure 7. Mitochondrial production of ROS in HeLa cells following treatment with compound **4i** (A, B) or compound **4n** (C, D). After 24 or 48 h incubations, cells were stained with H_2-DCFDA (A, C) or HE (B, D) and analyzed by flow cytometry. Data are presented as the mean ± SEM of three independent experiments.

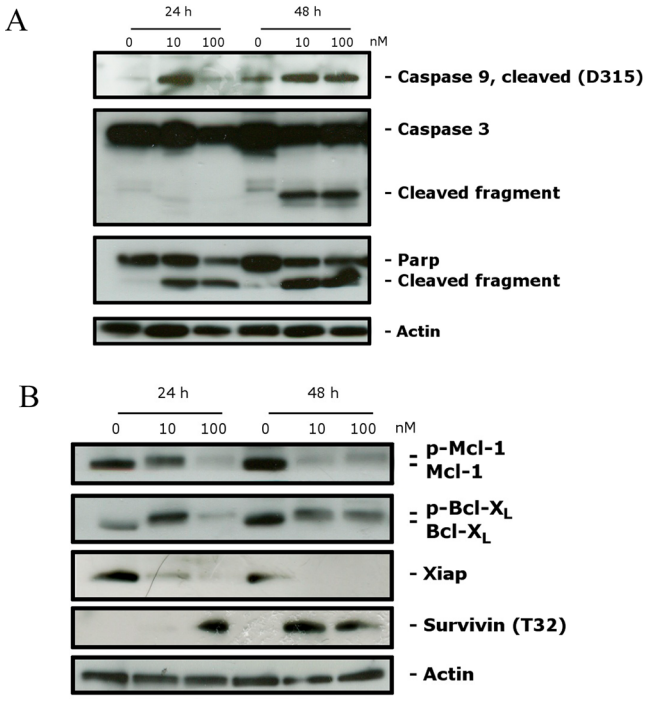

Figure 8. (A) Western blot analysis of caspase-3, cleaved caspase-9, and PARP after treatment of HeLa cells with **4i** at the indicated concentrations and for the indicated times. (B) Western blot analysis of Bcl-XL, survivin^{Thr32}, Mcl-1, and XIAP after treatment of HeLa cells with **4i** at the indicated concentrations and for the indicated times. To confirm equal protein loading, each membrane was stripped and reprobed with anti-β-actin antibody.

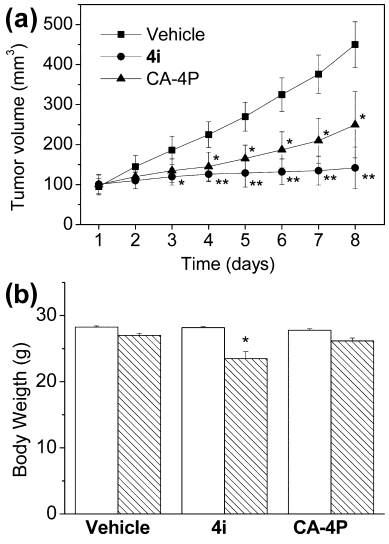

Figure 9. Inhibition of mouse allograft growth in vivo by compound **4i**. Male mice were injected subcutaneously at their dorsal region with 10^7 BNL 1MEA.7R.1 cells, a syngeneic hepatocellular carcinoma cell line. Tumor-bearing mice were administered the vehicle as a control or 5 mg/kg of **4i** or CA-4P as a reference compound. Injections were given intraperitoneally daily starting on day 1. The figure shows the average measured tumor volumes (A) and body weights of the mice (B) recorded at the end of the treatments. Data are presented as the mean ± SEM of tumor volume and body weight at each time point for five animals per group. Key: *, $p < 0.05$ vs control; **, $p < 0.01$ vs control.

reduction by the end of the observation period as compared with administration of vehicle only. The reduction in tumor growth was statistically significant as early as the third day after the beginning of the treatment, suggesting a rapid, effective delivery of the compound to the tumor mass. The effect on tumor volume reduction by **4i** was greater than that obtained with CA-4P, which caused a 44.5% reduction in volume at the end of the treatment. During the treatment period, only a small decrease in body weight occurred in the **4i**-treated animals (Figure 9B).

dx.doi.org/10.1021/jm400043d | J. Med. Chem. 2013, 56, 2606−2618

CONCLUSIONS

Manipulation of the scaffold of compounds with general structures **2** and **3** led to the successful identification of a new series of inhibitors of tubulin assembly, characterized by an ester and a 3,4,5-trimethoxyaniline function at the 2- and 3-positions, respectively, of the benzo[*b*]thiophene nucleus. Structure−activity relationship studies revealed that a methyl or methoxy substitution at the C-6 position of the benzo[*b*]-thiophene skeleton results in the greatest inhibitory effects on cancer cell growth (compounds **4f**, **4g**, **4i**, and **4j**). We also observed effects at the C-7 position, where the substitution of a methyl with a methoxy group (**4f** and **4k**, respectively) caused a substantial increase in activity. Comparing compounds **4i** and **4k** demonstrated that moving the methoxy group from the C-6 to the C-7 position caused a 4−130-fold reduction in antiproliferative activity.

The substitution with a nitrogen of the carbon at the C-6 position of compound **4f**, to furnish **4n**, resulted in improvement of the IC_{50} values, with 2−50-fold elevation in potency against four cancer cell lines. Compound **4n** was one of the most active antiproliferative agents and the most effective inhibitor of tubulin polymerization among the newly synthesized compounds. Its antitubulin activity closely paralleled that of reference compound **1**, and **4n** was more active than **1** as an inhibitor of cancer cell growth.

Moreover, **4i** and **4n** had very low toxicity toward both quiescent and mitogen-stimulated cultures of primary lymphocytes, suggesting that these compounds may have selectivity against cancer cells. Further experiments in other non cancer cell models are needed to confirm this finding. In additional experiments, we found that these compounds overcame drug resistance, since **4i** and **4n** were not substrates of P-gp and were active in a cell line with a mutant α-tubulin. Both **4i** and **4n** were potent inducers of apoptosis in the HeLa cell line. These compounds were able to induce Bcl-XL phosphorylation, which is associated with the loss of antiapoptotic functions. Another prosurvival protein, Mcl-1, was found to be phosphorylated in response to cell treatment with **4i**. Our results confirm that the induction of apoptosis by **4i** and **4n** is associated with dissipation of the mitochondrial transmembrane potential and activation of caspase-9 and caspase-3, which is coupled with terminal events of apoptosis, including PARP cleavage. The antitumor efficacy of **4i** was demonstrated in a syngeneic tumor model in mice, in which we observed a significant inhibition of tumor growth at a low dose of **4i**, which had minimal toxicity. In conclusion, our results demonstrated that **4i** is a very promising new tubulin binding agent and is worthy of further evaluation as a potential chemotherapeutic agent.

EXPERIMENTAL SECTION

Chemistry. *Materials and Methods.* ^{1}H NMR data were determined in $CDCl_3$ or DMSO-d_6 solutions with a Varian VXR 200 spectrometer or a Varian Mercury Plus 400 spectrometer. Peak positions are given in parts per million (δ) downfield from tetramethylsilane as an internal standard, and J values are given in hertz. Positive-ion electrospray ionization (ESI) mass spectra were recorded on a double-focusing Finnigan MAT 95 instrument with BE geometry. Melting points (mp's) were determined on a Buchi-Tottoli apparatus and are uncorrected. The purity of the tested compounds was determined by combustion elemental analyses conducted by the Microanalytical Laboratory of the Chemistry Department of the University of Ferrara with a Yanagimoto MT-5 CHN recorder elemental analyzer. All tested compounds yielded data consistent with a purity of at least 95% as compared with the theoretical values. All reactions were carried out under an inert atmosphere of dry nitrogen, unless otherwise indicated. Reaction courses and product mixtures were routinely monitored by TLC on silica gel (precoated F_{254} Merck plates), and compounds were visualized with aqueous $KMnO_4$. Flash chromatography was performed using 230−400 mesh silica gel and the indicated solvent system. Organic solutions were dried over anhydrous Na_2SO_4. All chemicals and reagents were purchased from Aldrich (Sigma-Aldrich) or Alfa Aesar (Johnson Matthey Co.).

*General Procedure A for the Synthesis of Compounds **6a−n**.* To a cold solution (−5 °C) containing the appropriate 2-nitrobenzonitrile **5a−g** or 2-chloro-3-cyanopyridine **5h,i** (5 mmol) and methyl/ethyl thioglycolate (5 mmol) in DMF (5 mL) was added dropwise a solution of KOH (1.12 g, 20 mmol, 4 equiv) in water (2.5 mL). The mixture was stirred at 0 °C for 1 h and added to ice water. The mixture was extracted with dichloromethane (3 × 15 mL), and the combined organic extracts were washed with water (2 × 5 mL) and brine, dried over Na_2SO_4, filtered, and concentrated under reduced pressure. The resulting residue was purified by column chromatography on silica gel to give **6a−n**.

*General Procedure B for the Synthesis of 3-Compounds **7a−n**.* In a dry three-neck round-bottom flask, anhydrous $CuBr_2$ (536 mg, 2.4 mmol) and *tert*-butyl nitrite (360 μL, 3 mmol) were dissolved in anhydrous acetonitrile (10 mL) under an Ar atmosphere. The resulting mixture was warmed at 65 °C and the appropriate derivative **6a−n** (2 mmol) in acetonitrile (5 mL) was slowly added. The reaction was complete after 2 h, as monitored by TLC. The dark mixture was allowed to reach room temperature, poured into a saturated aqueous NH_4Cl solution (10 mL), and extracted with CH_2Cl_2 (30 mL). The organic phase was washed twice with a saturated aqueous NH_4Cl solution (10 mL) and brine (10 mL), dried over Na_2SO_4, and concentrated at reduced pressure to furnish a residue that was purified by flash chromatography on silica gel to give **7a−n**.

*General Procedure C for the Preparation of Compounds **4a−n**.* A dry Schlenk tube was charged with dry toluene (5 mL), the appropriate bromo derivative **7a−n** (0.5 mmol), $Pd(OAc)_2$ (13 mol %, 15 mg), *rac*-BINAP (4 mol %, 15 mg), $CsCO_3$ (230 mg, 0.7 mmol, 1.4 equiv), and 3,4,5-trimethoxyaniline (137 mg, 0.75 mmol, 1.5 equiv) under Ar, and the mixture was heated at 100 °C for 18 h. After cooling, the mixture was filtered through a pad of Celite and the filtrate diluted with EtOAc (10 mL) and water (5 mL). The organic phase was washed with brine (5 mL), dried over Na_2SO_4, and concentrated under vacuum. The residue was purified by column chromatography on silica gel to furnish **4a−n**.

*Methyl 3-[(3,4,5-Trimethoxyphenyl)amino]-1-benzo[b]-thiophene-2-carboxylate (**4a**).* Following general procedure C, the crude residue was purified by flash chromatography, using ethyl acetate/petroleum ether (2:8, v/v) as the eluting solution, to furnish **4a** as a yellow solid (78% yield), mp 160−161 °C. ^{1}H NMR ($CDCl_3$): δ 3.73 (s, 6H), 3.85 (s, 3H), 3.92 (s, 3H), 6.33 (s, 2H), 7.12 (m, 1H), 7.46 (m, 2H), 7.82 (d, J = 8.0 Hz, 1H), 8.83 (s, 1H). ^{13}C NMR ($CDCl_3$): δ 52.0, 56.2 (2×), 61.2, 99.8 (2×), 105.5, 123.3, 123.4, 125.9, 127.9, 131.7, 138.1 (2×), 140.2, 146.5, 153.6 (2×), 166.0. MS (ESI): $[M + 1]^+$ = 374.1. Anal. ($C_{19}H_{19}NO_5S$) C, H, N.

*Ethyl 3-[(3,4,5-tTrimethoxyphenyl)amino]-1-benzo[b]thiophene-2-carboxylate (**4b**).* Following general procedure C, the crude residue was purified by flash chromatography, using ethyl acetate/petroleum ether (2:8, v/v) as the eluting solution, to furnish **4b** as a yellow solid (>95% yield), mp 120−121 °C. ^{1}H NMR ($CDCl_3$): δ 1.41 (t, J = 7.4 Hz, 3H), 3.72 (s, 6H), 3.85 (s, 3H), 4.40 (q, J = 7.2 Hz, 2H), 6.32 (s, 2H), 7.17 (m, 1H), 7.42 (m, 2H), 7.77 (d, J = 8.0 Hz, 1H), 8.81 (s, 1H). ^{13}C NMR ($CDCl_3$): δ 14.5, 56.1 (2×), 61.0, 61.2, 99.7 (2×), 110.3, 123.3, 123.4, 125.9, 127.8, 131.8, 134.5, 138.2, 140.2, 146.3, 153.6 (2×), 165.7. MS (ESI): $[M + 1]^+$ = 388.2. Anal. ($C_{20}H_{21}NO_5S$) C, H, N.

*Methyl 4-Methyl-3-[(3,4,5-trimethoxyphenyl)amino]-1-benzo[b]-thiophene-2-carboxylate (**4c**).* Following general procedure C, the crude residue was purified by flash chromatography, using ethyl acetate/petroleum ether (2:8, v/v) as the eluting solution, to furnish **4c** as a brown solid (56% yield), mp 192−194 °C. ^{1}H NMR ($CDCl_3$): δ 2.36 (s, 3H), 3.64 (s, 6H), 3.77 (s, 3H), 3.91 (s, 3H), 6.00 (s, 2H),

7.04 (d, J = 7.4 Hz, 1H), 7.35 (m, 1H), 7.61 (d, J = 8.0 Hz, 1H), 8.17 (s, 1H). ^{13}C NMR ($CDCl_3$): δ 20.2, 52.2, 56.0 (2×), 61.1, 95.3 (2×), 113.9, 120.8, 127.2, 127.9, 133.1, 133.6, 136.7, 140.4, 142.8, 146.7, 153.9 (2×), 165.3. MS (ESI): $[M + 1]^+$ = 388.0. Anal. ($C_{20}H_{21}NO_5S$) C, H, N.

*Ethyl 4-Methyl-3-[(3,4,5-trimethoxyphenyl)amino]-1-benzo[b]-thiophene-2-carboxylate (**4d**).* Following general procedure C, the crude residue was purified by flash chromatography, using ethyl acetate/petroleum ether (2:8, v/v) as the eluting solution, to furnish **4d** as a yellow solid (48% yield), mp 120−122 °C. ^{1}H NMR ($CDCl_3$): δ 1.36 (t, J = 7.0 Hz, 3H), 2.36 (s, 3H), 3.61 (s, 6H), 3.77 (s, 3H), 4.35 (q, J = 7.2 Hz, 2H), 6.00 (s, 2H), 7.02 (d, J = 7.4 Hz, 1H), 7.36 (m, 1H), 7.62 (d, J = 7.6 Hz, 1H), 8.18 (s, 1H). ^{13}C NMR ($CDCl_3$): δ 14.4, 20.1, 56.0 (2×), 61.1, 61.3, 95.3 (2×), 114.4, 120.8, 126.1, 127.2, 127.8, 133.7, 136.7, 140.4, 142.9, 146.5, 153.9 (2×), 164.9. MS (ESI): $[M + 1]^+$ = 402.0. Anal. ($C_{21}H_{23}NO_5S$) C, H, N.

*Methyl 5-Methyl-3-[(3,4,5-trimethoxyphenyl)amino]-1-benzo[b]-thiophene-2-carboxylate (**4e**).* Following general procedure C, the crude residue was purified by flash chromatography, using ethyl acetate/petroleum ether (2:8, v/v) as the eluting solution, to furnish **4e** as a yellow solid (73% yield), mp 190−192 °C. ^{1}H NMR ($CDCl_3$): δ 2.29 (s, 3H), 3.73 (s, 6H), 3.84 (s, 3H), 3.91 (s, 3H), 6.31 (s, 2H), 7.23 (d, J = 7.8 Hz, 1H), 7.27 (s, 1H), 7.65 (d, J = 7.8 Hz, 1H), 8.77 (s, 1H). ^{13}C NMR ($CDCl_3$): δ 21.5, 51.9, 56.2 (2×), 61.2, 99.4 (2×), 106.3, 122.9, 125.5, 129.8, 132.1, 133.3, 134.4, 137.5, 138.2, 146.0, 153.5 (2×), 166.0. MS (ESI): $[M + 1]^+$ = 388.0. Anal. ($C_{20}H_{21}NO_5S$) C, H, N.

*Methyl 6-Methyl-3-[(3,4,5-trimethoxyphenyl)amino]-1-benzo[b]-thiophene-2-carboxylate (**4f**).* Following general procedure C, the crude residue was purified by flash chromatography, using ethyl acetate/petroleum ether (2:8, v/v) as the eluting solution, to furnish **4f** as a yellow solid (64% yield), mp 168−170 °C. ^{1}H NMR ($CDCl_3$): δ 2.43 (s, 3H), 3.73 (s, 6H), 3.84 (s, 3H), 3.91 (s, 3H), 6.33 (s, 2H), 7.02 (d, J = 8.6 Hz, 1H), 7.31 (d, J = 8.6 Hz, 1H), 7.53 (s, 1H), 8.80 (s, 1H). ^{13}C NMR ($CDCl_3$): δ 21.7, 51.9, 56.2 (2×), 61.2, 99.9 (2×), 104.3, 123.0, 125.3, 125.6, 129.5, 134.6, 138.1, 138.4, 140.7, 146.6, 153.5 (2×), 166.1. MS (ESI): $[M + 1]^+$ = 388.0. Anal. ($C_{20}H_{21}NO_5S$) C, H, N.

*Ethyl 6-Methyl-3-[(3,4,5-trimethoxyphenyl)amino]-1-benzo[b]-thiophene-2-carboxylate (**4g**).* Following general procedure C, the crude residue was purified by flash chromatography, using ethyl acetate/petroleum ether (2:8, v/v) as the eluting solution, to furnish **4g** as a yellow solid (79% yield), mp 125−127 °C. ^{1}H NMR ($CDCl_3$): δ 1.37 (t, J = 7.0 Hz, 3H), 2.43 (s, 3H), 3.73 (s, 6H), 3.84 (s, 3H), 4.39 (q, J = 7.0 Hz, 2H), 6.32 (s, 2H), 6.96 (d, J = 8.4 Hz, 1H), 7.31 (d, J = 8.6 Hz, 1H), 7.53 (s, 1H), 8.82 (s, 1H). ^{13}C NMR ($CDCl_3$): δ 14.5, 21.8, 56.1 (2×), 60.9, 61.2, 99.7 (2×), 104.9, 121.7, 122.9, 125.3, 125.5, 129.6, 138.2, 138.3, 140.6, 146.4, 153.5 (2×), 165.8.. MS (ESI): $[M + 1]^+$ = 402.2. Anal. ($C_{21}H_{23}NO_5S$) C, H, N.

*Methyl 7-Methyl-3-[(3,4,5-trimethoxyphenyl)amino]-1-benzo[b]-thiophene-2-carboxylate (**4h**).* Following general procedure C, the crude residue was purified by flash chromatography, using ethyl acetate/petroleum ether (2:8, v/v) as the eluting solution, to furnish **4h** as a cream-colored solid (70% yield), mp 170−172 °C. ^{1}H NMR ($CDCl_3$): δ 2.52 (s, 3H), 3.72 (s, 6H), 3.85 (s, 3H), 3.93 (s, 3H), 6.34 (s, 2H), 7.10 (m, 1H), 7.33 (m, 2H), 8.80 (s, 1H). ^{13}C NMR ($CDCl_3$): δ 19.7, 52.0, 56.1 (2×), 61.2, 99.8 (2×), 102.4, 123.6, 123.9, 127.9, 131.6, 132.5, 124.6, 138.1, 140.4, 147.2, 153.5 (2×), 166.1. MS (ESI): $[M + 1]^+$ = 388.0. Anal. ($C_{20}H_{21}NO_5S$) C, H, N.

*Methyl 6-Methoxy-3-[(3,4,5-trimethoxyphenyl)amino]-1-benzo-[b]thiophene-2-carboxylate (**4i**).* Following general procedure C, the crude residue was purified by flash chromatography, using ethyl acetate/petroleum ether (2:8, v/v) as the eluting solution, to furnish **4i** as a yellow solid (78% yield), mp 155−156 °C. ^{1}H NMR ($CDCl_3$): δ 3.73 (s, 6H), 3.84 (s, 3H), 3.87 (s, 3H), 3.90 (s, 3H), 6.34 (s, 2H), 6.76 (dd, J = 9.2 and 2.4 Hz, 1H), 7.16 (d, J = 2.4 Hz, 1H), 7.30 (d, J = 9.2 Hz, 1H), 8.81 (s, 1H). ^{13}C NMR ($CDCl_3$): δ 51.8, 55.6, 56.1 (2×), 61.2, 100.0 (2×), 104.7, 113.3, 114.1, 125.4, 126.8, 137.9, 138.2, 142.5, 146.7, 153.5 (2×), 159.9, 166.0. MS (ESI): $[M + 1]^+$ = 404.2. Anal. ($C_{20}H_{21}NO_6S$) C, H, N.

*Ethyl 6-Methoxy-3-[(3,4,5-trimethoxyphenyl)amino]-1-benzo[b]-thiophene-2-carboxylate (**4j**).* Following general procedure C, the crude residue was purified by flash chromatography, using ethyl acetate/petroleum ether (2:8, v/v) as the eluting solution, to furnish **4j** as a yellow solid (69% yield), mp 155−157 °C. ^{1}H NMR ($CDCl_3$): δ 1.40 (t, J = 7.2 Hz, 3H), 3.75 (s, 6H), 3.81 (s, 3H), 3.87 (s, 3H), 4.36 (q, J = 7.2 Hz, 2H), 6.33 (s, 2H), 6.84 (dd, J = 9.0 and 2.4 Hz, 1H), 7.14 (d, J = 2.4 Hz, 1H), 7.32 (d, J = 9.0 Hz, 1H), 8.80 (s, 1H). ^{13}C NMR ($CDCl_3$): δ 14.6, 55.6, 56.2 (2×), 60.8, 61.2, 99.9 (2×), 104.7, 110.1, 114.0, 125.5, 126.8, 130.5, 134.6, 138.1, 142.4, 153.6 (2×), 159.9, 165.6. MS (ESI): $[M + 1]^+$ = 418.1. Anal. ($C_{21}H_{23}NO_6S$) C, H, N.

*Methyl 7-Methoxy-3-[(3,4,5-trimethoxyphenyl)amino]-1-benzo-[b]thiophene-2-carboxylate (**4k**).* Following general procedure C, the crude residue was purified by flash chromatography, using ethyl acetate/petroleum ether (2:8, v/v) as the eluting solution, to furnish **4k** as a yellow solid (74% yield), mp 176−178 °C. ^{1}H NMR ($CDCl_3$): δ 3.72 (s, 6H), 3.84 (s, 3H), 3.92 (s, 3H), 3.99 (s, 3H), 6.33 (s, 2H), 6.80 (dd, J = 7.2 and 1.4 Hz, 1H), 7.06 (m, 2H), 8.76 (s, 1H). ^{13}C NMR ($CDCl_3$): δ 52.0, 55.8, 56.1 (2×), 61.2, 99.8 (2×), 104.2, 106.9, 118.4, 121.6, 124.8, 133.4, 134.5, 138.1, 146.8, 153.5 (2×), 154.5, 166.1. MS (ESI): $[M + 1]^+$ = 404.0. Anal. ($C_{20}H_{21}NO_6S$) C, H, N.

*Methyl 3-[(3,4,5-Trimethoxyphenyl)amino]thieno[2,3-b]pyridine-2-carboxylate (**4l**).* Following general procedure C, the crude residue was purified by flash chromatography, using ethyl acetate/petroleum ether (3:7, v/v) as the eluting solution, to furnish **4l** as a yellow solid (52% yield), mp 176−178 °C. ^{1}H NMR ($CDCl_3$): δ 3.74 (s, 6H), 3.86 (s, 3H), 3.94 (s, 3H), 6.35 (s, 2H), 7.09 (m, 1H), 7.61 (dd, J = 8.4 and 1.6 Hz, 1H), 8.61 (dd, J = 4.4 and 1.6 Hz, 1H), 8.88 (s, 1H). ^{13}C NMR ($CDCl_3$): δ 52.1, 56.2 (2×), 61.2, 100.6 (2×), 110.3, 118.4, 125.6, 133.5, 135.3, 137.4, 144.6, 145.7, 150.3, 153.8 (2×), 166.0. MS (ESI): $[M + 1]^+$ = 375.1. Anal. ($C_{18}H_{18}N_2O_5S$) C, H, N.

*Ethyl 3-[(3,4,5-Trimethoxyphenyl)amino]thieno[2,3-b]pyridine-2-carboxylate (**4m**).* Following general procedure C, the crude residue was purified by flash chromatography, using ethyl acetate/petroleum ether (3:7, v/v) as the eluting solution, to furnish **4m** as a yellow solid (76% yield), mp 167−168 °C. ^{1}H NMR ($CDCl_3$): δ 1.42 (t, J = 7.2 Hz, 3H), 3.74 (s, 6H), 3.86 (s, 3H), 4.42 (q, J = 7.2 Hz, 2H), 6.34 (s, 2H), 7.09 (m, 1H), 7.62 (dd, J = 8.2 and 1.6 Hz, 1H), 8.62 (dd, J = 4.6 and 1.6 Hz, 1H), 8.90 (s, 1H). ^{13}C NMR ($CDCl_3$): δ14.5, 56.2 (2×), 61.2, 61.3, 100.4 (2×), 104.4, 118.4, 125.7, 133.4, 135.2, 137.5, 144.4, 150.2, 153.7 (2×), 161.1, 165.7. MS (ESI): $[M + 1]^+$ = 389.1. Anal. ($C_{19}H_{20}N_2O_5S$) C, H, N.

*Methyl 6-Methyl-3-[(3,4,5-trimethoxyphenyl)amino]thieno[2,3-b]pyridine-2-carboxylate (**4n**).* Following general procedure C, the crude residue was purified by flash chromatography, using ethyl acetate/petroleum ether (3:7, v/v) as the eluting solution, to furnish **4n** as a yellow solid (63% yield), mp 186−188 °C. ^{1}H NMR ($CDCl_3$): δ 2.64 (s, 3H), 3.74 (s, 6H), 3.85 (s, 3H), 3.92 (s, 3H), 6.34 (s, 2H), 6.93 (d, J = 8.6 Hz, 1H), 7.50 (d, J = 8.6 Hz, 1H), 8.88 (s, 1H). ^{13}C NMR ($CDCl_3$): δ 24.8, 52.0, 56.2 (2×), 61.2, 100.5 (2×), 102.1, 118.8, 122.3, 133.5, 135.2, 137.4, 144.8, 145.3, 153.7 (2×), 160.1, 166.2. MS (ESI): $[M + 1]^+$ = 389.0. Anal. ($C_{19}H_{20}N_2O_5S$) C, H, N.

Antiproliferative Assays. Human T-cell leukemia (Jurkat), human B-cell leukemia (SEM), and human promyelocytic leukemia (HL-60) cells were grown in RPMI-1640 medium (Gibco, Milano, Italy). Breast adenocarcinoma (MCF-7), human non-small-cell lung carcinoma (A549), human cervix carcinoma (HeLa), and human colon adenocarcinoma (HT-29) cells were grown in DMEM medium (Gibco). Both media were supplemented with 115 units/mL penicillin G (Gibco), 115 μg/mL streptomycin (Invitrogen, Milano, Italy), and 10% fetal bovine serum (Invitrogen). These cell lines were purchased from ATCC. CEM$^{Vbl\text{-}100}$ cells are a multi-drug-resistant line selected against vinblastine.[24] LoVo^{Doxo} cells are a doxorubicin-resistant subclone of LoVo cells[25] and were grown in complete Ham's F12 medium supplemented with doxorubicin (0.1 μg/mL). LoVo^{Doxo} and CEM$^{Vbl\text{-}100}$ were a kind gift of Dr. G. Arancia (Istituto Superiore di Sanità, Rome, Italy). A549-T12 cells are a non-small-cell lung carcinoma line exhibiting resistance to paclitaxel[29] and were kindly donated by Prof. I. Castagliuolo (University of Padova). They were

dx.doi.org/10.1021/jm400043d | J. Med. Chem. 2013, 56, 2606−2618

grown in complete DMEM medium supplemented with paclitaxel (12 nM). Stock solutions (10 mM) of the different compounds were obtained by dissolving them in DMSO. Individual wells of a 96-well tissue culture microtiter plate were inoculated with 100 μL of complete medium containing 8×10^3 cells. The plates were incubated at 37 °C in a humidified 5% CO_2 incubator for 18 h prior to the experiments. After medium removal, 100 μL of fresh medium containing the test compound at different concentrations was added to each well and incubated at 37 °C for 72 h. The percentage of DMSO in the medium never exceeded 0.25%. This was also the maximum DMSO concentration in all cell-based assays described below. Cell viability was assayed by the 3-(4,5-dimethylthiazol-2-yl)-2,5-diphenyltetrazolium bromide test as previously described.[54] The IC_{50} was defined as the compound concentration required to inhibit cell proliferation by 50%, in comparison with cells treated with the maximum amount of DMSO (0.25%) and considered as 100% viable.

PBLs from healthy donors were obtained by separation on a Lymphoprep (Fresenius KABI Norge AS) gradient. After extensive washing, cells were resuspended (1.0×10^6 cells/mL) in RPMI-1640 with 10% fetal bovine serum and incubated overnight. For cytotoxicity evaluations in proliferating PBL cultures, nonadherent cells were resuspended at 5×10^5 cells/mL in growth medium, containing 2.5 μg/mL PHA (Irvine Scientific). Different concentrations of the test compounds were added, and viability was determined 72 h later by the MTT test. For cytotoxicity evaluations in resting PBL cultures, nonadherent cells were resuspended (5×10^5 cells/mL) and treated for 72 h with the test compounds, as described above.

Molecular Modeling. All molecular modeling studies were performed on a MacPro dual 2.66 GHz Xeon running Ubuntu. The tubulin structure was downloaded from the Protein Data Bank (http://www.rcsb.org/, PDB code 1SA0).[55] Hydrogen atoms were added to the protein, using Molecular Operating Environment (MOE),[56] and minimized keeping all the heavy atoms fixed until an RMSD gradient of 0.05 kcal mol^{-1} $Å^{-1}$ was reached. Ligand structures were built with MOE and minimized using the MMFF94x force field until an RMSD gradient of 0.05 kcal mol^{-1} $Å^{-1}$ was reached. The docking simulations were performed using PLANTS.[57]

Effects on Tubulin Polymerization and on Colchicine Binding to Tubulin. To evaluate the effect of the compounds on tubulin assembly in vitro,[30] varying concentrations of compounds were preincubated with 10 μM bovine brain tubulin in glutamate buffer at 30 °C and then cooled to 0 °C. After addition of 0.4 mM GTP, the mixtures were transferred to 0 °C cuvettes in a recording spectrophotometer and warmed to 30 °C. Tubulin assembly was followed turbidimetrically at 350 nm. The IC_{50} was defined as the compound concentration that inhibited the extent of assembly by 50% after a 20 min incubation. The ability of the test compounds to inhibit colchicine binding to tubulin was measured as described,[32] except that the reaction mixtures contained 1 μM tubulin, 5 μM [^{3}H]colchicine, and 1 or 5 μM test compound.

Flow Cytometric Analysis of Cell Cycle Distribution. For flow cytometric analysis of DNA content, 5×10^5 HeLa cells in exponential growth were treated with different concentrations of the test compounds for 24 and 48 h. After the incubation period, the cells were collected, centrifuged, and fixed with ice-cold ethanol (70%). The cells were treated with lysis buffer containing RNase A and 0.1% Triton X-100 and then stained with PI. Samples were analyzed on a Cytomic FC500 flow cytometer (Beckman Coulter). DNA histograms were analyzed using MultiCycle for Windows (Phoenix Flow Systems).

Annexin-V Assay. Surface exposure of PS on apoptotic cells was measured by flow cytometry with a Coulter Cytomics FC500 (Beckman Coulter) by adding annexin-V conjugated to fluorescein isothiocyanate (FITC) to cells according to the manufacturer's instructions (Annexin-V Fluos, Roche Diagnostic). Simultaneously, the cells were stained with PI. Excitation was set at 488 nm, and the emission filters were at 525 and 585 nm, respectively, for FITC and PI.

Assessment of Mitochondrial Changes. The mitochondrial membrane potential was measured with the lipophilic cationic dye JC-1 (Molecular Probes), as described.[54] The production of ROS was measured by flow cytometry using either HE (Molecular Probes) or H_2DCFDA (Molecular Probes), as previously described.[54]

Western Blot Analysis. HeLa cells were incubated in the presence of test compounds and, after different times, were collected, centrifuged, and washed two times with ice-cold phosphate-buffered saline (PBS). The pellet was then resuspended in lysis buffer. After the cells were lysed on ice for 30 min, the lysates were centrifuged at 15000*g* at 4 °C for 10 min. The protein concentration in the supernatant was determined using the BCA protein assay reagents (Pierce, Italy). Equal amounts of protein (20 μg) were resolved using sodium dodecyl sulfate–polyacrylamide gel electrophoresis (SDS–PAGE) (7.5–15% acrylamide gels) and transferred to PVDF Hybond-p membranes (GE Healthcare). The membranes were blocked with I-block (Tropix), the membrane being gently rotated overnight at 4 °C. The membranes were then incubated with primary antibodies against Bcl-XL, Mcl-1, Xiap, p-survivin (Thr34), PARP, cleaved caspase-9, p-cdc2^{Tyr15}, cdc25c (Cell Signaling), caspase-3 (Alexis), cyclin B (Upstate), or β-actin (Sigma-Aldrich) for 2 h at room temperature. The membranes were next incubated with peroxidase-labeled secondary antibodies for 60 min. All membranes were visualized using ECL Advance (GE Healthcare) and exposed to Hyperfilm MP (GE Healthcare). To ensure equal protein loading, each membrane was stripped and reprobed with anti-β-actin antibody.

Antitumor Activity in Vivo. The in vivo cytotoxic activity of compound **4i** was investigated using a syngeneic murine hepatocellular carcinoma cell line (BNL 1ME A.7R.1) in Balb/c mice.[53] Male mice, 8 weeks old, were purchased from Harlan (S. Pietro al Natisone Udine, Italy), and tumors were induced by a subcutaneous injection in their dorsal region of 10^7 cells in 200 μL of sterile PBS. The animals were randomly divided into three groups, and starting on the second day, they were daily dosed intraperitoneally (ip) with 7 μL/kg free vehicle (0.9% NaCl containing 5% polyethylene glycol 400 and 0.5% Tween 80), compound **4i**, or the reference compound CA-4P, both at the dose of 5 mg/kg of body mass. Tumor sizes were measured daily for 7 days using a pair of calipers. In particular, the tumor volume (V) was calculated by the rotational ellipsoid formula: $V = AB^2/2$, where A is the longer diameter (axial) and B is the shorter diameter (rotational). All experimental procedures followed guidelines recommended by the Institutional Animal Care and Use Committee of Padova University.

Statistical Analysis. Unless indicated otherwise, the results are presented as the mean ± SEM. The differences between different treatments were analyzed using the two-sided Student's t test. P values of less than 0.05 were considered significant.

■ ASSOCIATED CONTENT

Ⓢ Supporting Information

Detailed characterization of synthesized compounds **6a–n** and **7a–n** and molecular modeling studies of **4f**, **4g**, **4h**, **4i**, **4j**, **4k**, and **4n** (Figure 1s). This material is available free of charge via the Internet at http://pubs.acs.org

■ AUTHOR INFORMATION

Corresponding Author

*Phone: 39-(0)532-455303 (R.R.); 39-(0)532-455293 (P.G.B.); 39-(0)49-8211451 (G.V.). Fax: 39-(0)532-455953 (R.R.); 39-(0)532-455953 (P.G.B.); 39-(0)49-8211462 (G.V.). E-mail: rmr@unife.it (R.R.); pgb@unife.it (P.G.B.); giampietro.viola1@unipd.it (G.V.).

Notes

The authors declare no competing financial interest.

■ ACKNOWLEDGMENTS

We thank Dr. Alberto Casolari for excellent technical assistance.

ABBREVIATIONS USED

CA-4, combretastatin A-4; CA-4P, combretastatin A-4 phosphate; DMF, *N*,*N*-dimethylformamide; KOH, potassium hydroxide; *t*BuONO, *tert*-butyl nitrite; $CuBr_2$, copper(II) bromide; $Pd(OAc)_2$, palladium(II) acetate; BINAP, *rac*-2,2′-bis(diphenylphosphane)-1,1′-binaphtyl; $CsCO_3$, cesium carbonate; *J*, coupling constant (in NMR spectroscopy); PBL, peripheral blood lymphocyte; PHA, phytohemaglutinin; FITC, fluorescein isothiocyanate; PI, propidium iodide; PS, phosphatidylserine; $\Delta\psi_{mt}$, mitochondrial transmembrane potential; JC-1, 5,5′,6,6′-tetrachloro-1,1′,3,3′-tetraethylbenzimidazolcarbocyanine; ROS, reactive oxygen species; HE, hydroxyethidine; H_2DCFDA, 2,7-dichlorodihydrofluorescein diacetate; PARP, poly(ADP-ribose) polymerase; IAP, inhibitor of apoptosis protein; HBSS, Hank's balanced salt solution; PBS, phosphate-buffered saline; SDS−PAGE, sodium dodecyl sulfate−polyacrylamide gel electrophoresis

REFERENCES

(1) Amos, L. A. Microtubule structure and its stabilisation. *Org. Biomol. Chem.* **2004**, *2*, 2153−2160.

(2) Walczak, C. E. Microtubule dynamics and tubulin interacting proteins. *Curr. Opin. Cell Biol.* **2000**, *12*, 52−56.

(3) Dumontet, C.; Jordan, M. A. Microtubule-binding agents: a dynamic field of cancer therapeutics. *Nat. Rev. Drug Discovery* **2010**, *9*, 790−803.

(4) Perez, E. A. Microtubule inhibitors: differentiating tubulin inhibiting agents based on mechanisms of action, clinical activity, and resistance. *Mol. Cancer Ther.* **2009**, *8*, 2086−2095.

(5) Carlson, R. O. New tubulin targeting agents currently in clinical development. *Expert Opin. Invest. Drugs* **2008**, *17*, 707−722.

(6) Pellegrini, F.; Budman, D. R. Review: tubulin function, action of antitubulin drugs, and new drug development. *Cancer Invest.* **2005**, *23*, 264−273.

(7) Yue, Q.-X.; Liu, X.; Guo, D.-A. Microtubule-binding natural products for cancer therapy. *Planta Med.* **2010**, *76*, 1037−1043.

(8) Lee, J. F.; Harris, L. N. Antimicrotubule agents. In *Cancer Principles & Practice of Oncology*, 8th ed.; DeVita, V. T., Jr., Lawrence, T. S., Rosenberg, S. A., Eds.; Lippincott Williams & Wilkins: Philadelphia, PA, 2008; pp 447−456.

(9) Pettit, G. R.; Singh, S. B.; Hamel, E.; Lin, C. M.; Alberts, D. S.; Garcia-Kendall, D. Isolation and structure of the strong cell growth and tubulin inhibitor combretastatin A-4. *Experentia* **1989**, *45*, 209−211.

(10) Lin, C. M.; Ho, H. H.; Pettit, G. R.; Hamel, E. Antimitotic natural products combretastatin A-4 and combretastatin A-2: studies on the mechanism of their inhibition of the binding of colchicine to tubulin. *Biochemistry* **1989**, *28*, 6984−6991.

(11) McGown, A. T.; Fox, B. W. Differential cytotoxicity of combretastatins A1 and A4 in two daunorubucin-resistant P388 cell lines. *Cancer Chemother. Pharmacol.* **1990**, *26*, 79−81.

(12) Siemann, D. W.; Chaplin, D. J.; Walicke, P. A. A review and update of the current status of the vasculature-disabling agent combretastatin-A4 phosphate (CA4P). *Expert Opin. Invest. Drugs* **2009**, *18*, 189−197.

(13) Romagnoli, R.; Baraldi, P. G.; Lopez Cara, C.; Hamel, E.; Basso, G.; Bortolozzi, R.; Viola, G. Synthesis and biological evaluation of 2-(3′,4′,5′-trimethoxybenzoyl)-3-aryl/arylaminobenzo[*b*]thiophene derivatives as a novel class of antiproliferative agents. *Eur. J. Med. Chem.* **2010**, *45*, 5781−5791.

(14) De Martino, G.; La Regina, G.; Coluccia, A.; Edler, M. C.; Barbera, M. C.; Brancale, A.; Wilcox, E.; Hamel, E.; Artico, M.; Silvestri, R. Arylthioindoles, potent inhibitors of tubulin polymerization. *J. Med. Chem.* **2004**, *47*, 6120−6123.

(15) De Martino, G.; Edler, M. C.; La Regina, G.; Coluccia, A.; Barbera, M. C.; Barrow, D.; Nicholson, R. I.; Chiosis, G.; Brancale, A.; Hamel, E.; Artico, M.; Silvestri, R. New arylthioindoles: potent inhibitors of tubulin polymerization. 2. Structure-activity relationships and molecular modeling studies. *J. Med. Chem.* **2006**, *49*, 947−954.

(16) La Regina, G.; Sarkar, T.; Bai, R.; Edler, M. C.; Saletti, R.; Coluccia, A.; Piscitelli, F.; Minelli, L.; Gatti, V.; Mazzoccoli, C.; Palermo, V.; Mazzoni, C.; Falcone, C.; Scovassi, A. I.; Giansanti, V.; Campiglia, P.; Porta, A.; Maresca, B.; Hamel, E.; Brancale, A.; Novellino, E.; Silvestri, R. New arylthioindoles and related bioisosteres at the sulfur bridging group. 4. Synthesis, tubulin polymerization, cell growth inhibition, and molecular modeling studies. *J. Med. Chem.* **2009**, *52*, 7512−7527.

(17) Gaukroger, K.; Hadfield, J. A.; Lawrence, N. J.; Nolan, S.; McGown, A. T. Structural requirements for the interaction of combretastatins with tubulin: how important is the trimethoxy unit? *Org. Biomol. Chem.* **2003**, *1*, 3033−3037.

(18) Hatanaka, T.; Fujita, K.; Ohsumi, K.; Nakagawa, R.; Fukuda, Y.; Nihei, Y.; Suga, Y.; Akiyama, Y.; Tsuji, T. Novel B-ring modified combretastatin analogues: synthesis and antineoplastic activity. *Bioorg. Med. Chem. Lett.* **1998**, *8*, 3371−3374.

(19) Beck, J. R. A direct synthesis of benzo[*b*]thiophene-2-carboxylate esters involving nitro displacement. *J. Org. Chem.* **1972**, *37*, 3224−3226.

(20) Doyle, M. P.; Siegfried, B.; Dellaria, J. F., Jr. Alkyl nitrite-metal halide deamination rections. 2. Substitutive deamination of arylamines by alkyl nitrites and copper (II) halides. A direct and remarkably efficient conversion of arylamines to aryl halides. *J. Org. Chem.* **1977**, *42*, 2426−2431.

(21) Queiroz, M.-J. R. P.; Begouin, A.; Ferreira, I. C. F. R.; Kirsch, G.; Calhelha, R. C.; Barbosa, S.; Estevinho, L. M. Palladium-catalysed amination of electron-deficient or relatively electron-rich benzo[*b*]-thienyl bromids—preliminary studies of antimicrobial activity and SARs. *Eur. J. Org. Chem.* **2004**, 3679−3685.

(22) Szakács, G.; Paterson, J. K.; Ludwig, J. A.; Booth-Genthe, C.; Gottesman, M. M. Targeting multidrug resistance in cancer. *Nat. Rev. Drug Discovery* **2006**, *5*, 219−234.

(23) Baguley, B. C. Multidrug resistance mechanism in cancer. *Mol. Biotechnol.* **2010**, *46*, 308−316.

(24) Dupuis, M.; Flego, M.; Molinari, A.; Cianfriglia, M. Saquinavir induces stable and functional expression of the multidrug transporter P-glycoprotein in human CD4 T-lymphoblastoid CEM rev cells. *HIV Med.* **2003**, *4*, 338−345.

(25) Toffoli, G.; Viel, A.; Tumiotto, I.; Biscontin, G.; Rossi, G.; Boiocchi, M. Pleiotropic-resistant phenotype is a multifactorial phenomenon in human colon carcinoma cell lines. *Br. J. Cancer* **1991**, *63*, 51−56.

(26) Verrills, N. M.; Kavallaris, M. Improving the targeting of tubulin-binding agents: lessons from drug resistance studies. *Curr. Pharm. Des.* **2005**, *11*, 1719−1733.

(27) Kavallaris, M. Microtubules and resistance to tubulin-binding agents. *Nat. Rev. Cancer* **2010**, *10*, 194−204.

(28) Ganguly, A.; Cabral, F. New insights into mechanisms of resistance to microtubule inhibitors. *Biochim. Biophys. Acta* **2011**, *1816*, 164−171.

(29) Martello, L. A.; Verdier-Pinard, P.; Shen, H. J.; He, L.; Torres, K.; Orr, G. A.; Horwitz, S. B. Elevated level of microtubule destabilizing factors in a taxol-resistant/dependent A549 cell line with an alpha-tubulin mutation. *Cancer Res.* **2003**, *63*, 1207−1213.

(30) Hamel, E. Evaluation of antimitotic agents by quantitative comparisons of their effects on the polymerization of purified tubulin. *Cell Biochem. Biophys.* **2003**, *38*, 1−21.

(31) Bhattacharyya, B.; Panda, D.; Gupta, S.; Banerjee, M. Antimitotic activity of colchicine and the structural basis for its interaction with tubulin. *Med. Res. Rev.* **2008**, *28*, 155−183.

(32) Verdier-Pinard, P.; Lai, J.-Y.; Yoo, H.-D.; Yu, J.; Marquez, B.; Nagle, D. G.; Nambu, M.; White, J. D.; Falck, J. R.; Gerwick, W. H.; Day, B. W.; Hamel, E. Structure-activity analysis of the interaction of curacin A, the potent colchicine site antimitotic agent, with tubulin and effects of analogs on the growth of MCF-7 breast cancer cells. *Mol. Pharmacol.* **1998**, *53*, 62−76.

(33) Massarotti, A.; Coluccia, A.; Silvestri, R.; Sorba, G.; Brancale, A. The tubulin colchicine domain: a molecular modeling perspective. *ChemMedChem* **2012**, *7*, 33−42.
(34) Coluccia, A.; Sabbadin, D.; Brancale, A. Molecular modelling studies on arylthioindoles as potent inhibitors of tubulin polymerization. *Eur. J. Med. Chem.* **2011**, *46*, 3519−3525.
(35) Clarke, P. R.; Allan, L. A. Cell-cycle control in the face of damage—a matter of life or death. *Trends Cell Biol.* **2009**, *19*, 89−98.
(36) Kiyokawa, H.; Ray, D. In vivo roles of Cdc25 phosphatases: biological insight into the anti-cancer therapeutic targets. *Anticancer Agents Med. Chem.* **2008**, *8*, 832−836.
(37) Donzelli, M.; Draetta, G. F. Regulating mammalian checkpoints through Cdc25 inactivation. *EMBO Rep.* **2003**, *4*, 671−677.
(38) Vermes, I.; Haanen, C.; Steffens-Nakken, H.; Reutelingsperger, C. A novel assay for apoptosis. Flow cytometric detection of phosphatidylserine expression on early apoptotic cells using fluorescein labelled annexin V. *J. Immunol. Methods* **1995**, *184*, 39−51.
(39) (a) Ly, J. D.; Grubb, D. R.; Lawen, A. The mitochondrial membrane potential ($\Delta\psi_m$) in apoptosis: an update. *Apoptosis* **2003**, *8*, 115−128. (b) Green, D. R.; Kroemer, G. The pathophysiology of mitochondrial cell death. *Science* **2004**, *305*, 626−629.
(40) (a) Cai, J.; Jones, D. P. Superoxide in apoptosis. Mitochondrial generation triggered by cytochrome *c* loss. *J. Biol. Chem.* **1998**, *273*, 11401−11404. (b) Nohl, H.; Gille, L.; Staniek, K. Intracellular generation of reactive oxygen species by mitochondria. *Biochem. Pharmacol.* **2005**, *69*, 719−723.
(41) Rothe, G.; Valet, G. Flow cytometric analysis of respiratory burst activity in phagocytes with hydroethidine and 2′,7′-dichlorofluorescein. *J. Leukocyte Biol.* **1990**, *47*, 440−448.
(42) (a) Chiu, W. H.; Luo, S. J.; Chen, C. L.; Cheng, J. H.; Hsieh, C. Y.; Wang, C. Y.; Huang, W. C.; Su, W. C.; Lin, C. F. Vinca alkaloids cause aberrant ROS-mediated JNK activation, Mcl-1 downregulation, DNA damage, mitochondrial dysfunction, and apoptosis in lung adenocarcinoma cells. *Biochem. Pharmacol.* **2012**, *83*, 1159−1171. (b) Mendez, G.; Policarpi, C.; Cenciarelli, C.; Tanzarella, C.; Antoccia, A. Role of Bim in apoptosis induced in H460 lung tumor cells by the spindle poison combretastatin-A4. *Apoptosis* **2011**, *16*, 940−949.
(43) Denault, J.-B.; Salvesen, G. S. Caspases: keys in the ignition of cell death. *Chem. Rev.* **2002**, *102*, 4489−4499.
(44) Porter, A. G.; Janicke, R. U. Emerging role of caspase-3 in apoptosis. *Cell Death Differ.* **1999**, *6*, 99−104.
(45) Mollinedo, F.; Gajate, C. Microtubules, microtubule-interfering agents and apoptosis. *Apoptosis* **2003**, *8*, 413−450.
(46) Poruchynsky, M. S.; Wang, E. E.; Rudin, C. M.; Blagosklonny, M. V.; Fojo, T. Bcl-xL is phosphorylated in malignant cells following microtubule disruption. *Cancer Res.* **1998**, *58*, 3331−3338.
(47) Matson, D. R.; Stukenberg, P. T. Spindle poisons and cell fate: a tale of two pathways. *Mol. Interventions* **2011**, *11*, 141−150.
(48) Wertz, I. E.; Kusam, S.; Lam, C.; Okamoto, T.; Sandoval, W.; Anderson, D. J.; Helgason, E.; Ernst, J. A.; Eby, M.; Liu, J.; Belmont, L. D.; Kaminker, J. S.; O'Rourke, K. M.; Pujara, K.; Kohli, P. B.; Johnson, A. R.; Chiu, M. L.; Lill, J. R.; Jackson, P. K.; Fairbrother, W. J.; Seshagiri, S.; Ludlam, M. J.; Leong, K. G.; Dueber, E. C.; Maecker, H.; Huang, D. C.; Dixit, V. M. Sensitivity to antitubulin chemotherapeutics is regulated by MCL1 and FBW7. *Nature* **2011**, *471*, 110−114.
(49) Harley, M. E.; Allan, L. A.; Sanderson, H. S.; Clarke, P. R. Phosphorylation of Mcl-1 by CDK1-cyclin B1 initiates its Cdc20-dependent destruction during mitotic arrest. *EMBO J.* **2010**, *29*, 2407−2420.
(50) Altieri, D. C.; Survivin, I. A. P. Proteins in cell-death mechanisms. *Biochem. J.* **2010**, *430*, 199−205.
(51) Castedo, M.; Perfettini, J. L.; Roumier, T.; Andreau, K.; Medema, R.; Kroemer, G. Cell death by mitotic catastrophe: a molecular definition. *Oncogene* **2004**, *23*, 2825−2837.
(52) O'Connor, D. S.; Grossman, D.; Plescia, J.; Li, F.; Zhang, H.; Villa, A.; Tognin, S.; Marchisio, P. C.; Altieri, D. C. Regulation of apoptosis at cell division by p34cdc2 phosphorylation of survivin. *Proc. Natl. Acad. Sci. U.S.A.* **2000**, *97*, 13103−13107.
(53) Gasparotto, V.; Castagliuolo, I.; Chiarelotto, G.; Pezzi, V.; Montanaro, D.; Brun, P.; Palù, G.; Viola, G.; Ferlin, M. G. Synthesis and biological activity of 7-phenyl-6,9-dihydro-3*H*-pyrrolo[3,2-*f*]-quinolin-9-ones: a new class of antimitotic agents devoid of aromatase activity. *J. Med. Chem.* **2006**, *49*, 1910−1915.
(54) Viola, G.; Vedaldi, D.; Dall'Acqua, F.; Fortunato, E.; Basso, G.; Bianchi, N.; Zuccato, C.; Borgatti, M.; Lampronti, I.; Gambari, R. Induction of γ-globin mRNA, erythroid differentiation and apoptosis in UVA-irradiated human erythroid cells in the presence of furocumarin derivatives. *Biochem. Pharmacol.* **2008**, *75*, 810−825.
(55) Ravelli, R. B. G.; Gigant, B.; Curmi, P. A.; Jourdain, I.; Lachkar, S.; Sobel, A.; Knossow, M. Insight into tubulin regulation from a complex with colchicine and a stathmin-like domain. *Nature* **2004**, *428*, 198−202.
(56) *Molecular Operating Environment (MOE 2010.10)*; Chemical Computing Group, Inc.: Montreal, Quebec, Canada. http://www.chemcomp.com (accessed February 23, 2013).
(57) Korb, O.; Stützle, T.; Exner, T. E. PLANTS: Application of ant colony optimization to structure-based drug design. In *Ant Colony Optimization and Swarm Intelligence*, 5th International Workshop, ANTS 2006, Brussels, Belgium, Sept 4−7, 2006; Dorigo, M., Gambardella, L. M., Birattari, M., Martinoli, A., Poli, R., Sttzle, T., Eds.; Springer: Berlin, 2006; LNCS 4150, pp 247−258.